Received: 3 November 2020 | Revised: 17 December 2020 | Accepted: 8 January 2021

DOI: 10.1002/ardp.202000414

FULL PAPER

ARCH PHARM DPhG
Archiv der Pharmazie

Synthesis, docking studies, and pharmacological evaluation of 2-hydroxypropyl-4-arylpiperazine derivatives as serotoninergic ligands

Elisa Magli[1] | Ewa Kędzierska[2] | Agnieszka A. Kaczor[3,4] | Anna Bielenica[5] | Beatrice Severino[1] | Ewa Gibuła-Tarłowska[2] | Jolanta H. Kotlińska[2] | Angela Corvino[1] | Rosa Sparaco[1] | Giovanna Esposito[1] | Stefania Albrizio[1] | Elisa Perissutti[1] | Francesco Frecentese[1] | Anna Leśniak[6] | Magdalena Bujalska-Zadrożny[6] | Marta Struga[5] | Raffaele Capasso[1] | Vincenzo Santagada[1] | Giuseppe Caliendo[1] | Ferdinando Fiorino[1]

[1]Dipartimento di Farmacia, Università degli Studi di Napoli "Federico II", Napoli, Italy

[2]Department of Pharmacology and Pharmacodynamics, Faculty of Pharmacy with Division of Medical Analytics, Medical University of Lublin, Lublin, Poland

[3]Department of Synthesis and Chemical Technology of Pharmaceutical Substances with Computer Modeling Laboratory, Faculty of Pharmacy, Medical University of Lublin, Lublin, Poland

[4]School of Pharmacy, University of Eastern Finland, Kuopio, Finland

[5]Department of Biochemistry, Medical University of Warsaw, Warsaw, Poland

[6]Department of Pharmacodynamics, Centre for Preclinical Research and Technology, Faculty of Pharmacy, Medical University of Warsaw, Warsaw, Poland

Correspondence
Ferdinando Fiorino, Dipartimento di Farmacia, Università degli Studi di Napoli "Federico II", Via D. Montesano, 49, 80131 Napoli, Italy.
Email: fefiorin@unina.it

Abstract

A new series of norbornene and *exo*-*N*-hydroxy-7-oxabicyclo[2.2.1]hept-5-ene-2,3-dicarboximide derivatives was prepared, and their affinities to the 5-HT_{1A}, 5-HT_{2A}, and 5-HT_{2C} receptors were evaluated and compared with a previously synthesized series of derivatives characterized by the same nuclei, to identify selective ligands for the subtype receptors. Arylpiperazines represent one of the most important classes of 5-HT_{1A}R ligands, and the research of new derivatives has been focused on the modification of one or more portions of this pharmacophore. The combination of structural elements (heterocyclic nucleus, hydroxyalkyl chain, and 4-substituted piperazine), known to be critical for the affinity to 5-HT_{1A} receptors, and the proper selection of substituents resulted in compounds with high specificity and affinity toward serotoninergic receptors. The most active compounds were selected for further in vivo assays to determine their functional activity. Finally, to rationalize the obtained results, molecular docking studies were performed. The results of the pharmacological studies showed that **3e**, **4j**, and **4n** were the most active and promising derivatives for the serotonin receptor considered in this study.

KEYWORDS

5-HT_{1A} receptor ligands, arylpiperazine derivatives, *exo*-*N*-hydroxy-7-oxabicyclo[2.2.1]hept-5-ene-2,3-dicarboximide, norbornene nucleus, serotonin

1 | INTRODUCTION

Serotonin (5-hydroxytryptamine, 5-HT) is an important neuromodulator in the central and peripheral nervous systems (CNS and PNS, respectively), which plays a critical role in a wide range of physiological and pathophysiological processes. Molecular cloning techniques, amino acid sequence determination, evaluation of its pharmacological properties, second messenger coupling, and signal transduction characterization have allowed the identification of at least seven classes (5-HT_{1-7}), with additional subclasses amounting to 15 receptors.[1] Whereas 5-HT_3Rs are cation-permeable ion channels, all the others are G-protein-coupled receptors (GPCRs) and are classified as rhodopsin-like receptors. Serotonin receptors (5-HTRs) are the most widespread targets of drugs due to the

numerous biological effects of the endogenous ligand; serotonin is mainly involved in impulsivity and alcoholism, and in the different phases of sleep, sexual behavior, appetite control, thermoregulation, and cardiovascular function.[2] In addition, it is already known that 5-HT plays a fundamental role as a growth factor in several types of nontumoral and tumoral cells, differentiation, and gene expression also related to oncogenes.[3] Consequently, pharmacological manipulation of the 5-HT system is assumed to have therapeutic potential, and therefore it has been the subject of intense research.[4]

Electrophysiological, pharmacological, and biochemical pieces of evidence have demonstrated that 5-HT_{1A}Rs, localized in primary afferent neurons, are involved in different neurological disorders and are also known to be implicated in the proliferation of human tumor cells; however, their function still remains poorly understood. 5-HT_{1A}R antagonists inhibit the growth of different prostatic tumor cell lines, such as PC-3, DU-145, and LNCaP, as well as the proliferation of PC-3 xenografted subcutaneously in athymic nude mice.[3] Concerning the 5-HT_2 receptor family (5-HT_{2A}, 5-HT_{2B}, and 5-HT_{2C}), 5-HT_{2A}Rs activation stimulates the secretion of various hormones and influences neuronal plasticity; peripheral 5-HT_{2A} receptors mediate several processes such as vasoconstriction and platelet aggregation.[5] 5-HT_{2C} receptor regulates physiological functions such as locomotory activity, anxiogenesis, and neuroendocrine functions, besides being involved in sexual dysfunction in males.[6,7]

Arylpiperazines are one of the most important classes of 5-HT_{1A}R ligands from which anxiolytics, including buspirone, antipsychotics, such as ziprasidone, perospirone, and aripiprazole, and several other pharmacological tools originated. The general structure of arylpiperazines consists of a terminal fragment containing an amide, imide, alkyl, arylalkyl, heteroarylalkyl, or tetralin function linked through a flexible aliphatic chain of variable length to the *N*-1-arylpiperazine moiety. The research of new derivatives has been focused on the modification of one or more portions of such a pharmacophore. Two main interactions prove to be important for the affinity of arylpiperazines for 5-HT_{1A}Rs: (a) an ionic bond between the protonated nitrogen atom of the piperazine ring and the carboxyl oxygen of the side chain of Asp3.32 and (b) an edge-to-face CH/π interaction between the aromatic ring and the Phe6.52 residue, which stabilizes the ligand binding. The basic pharmacophore of the 5-HT_{1A}R ligands is the same for agonists and antagonists, and it consists of an aromatic nucleus and a basic nitrogen atom, whose optimal distance is 5.2 Å, but the nitrogen atom lies at 0.2 Å above the plane defined by the reference ring.[1]

A limitation in the potential use of many 5-HTR_{1A} receptor ligands as drugs or pharmacological tools of many 5-HT_{1A} receptor ligands is their undesired high affinity for other receptors. The dopaminergic D_2 receptor and α_1-adrenoceptor are two other examples of receptors for which several 5-HT_{1A} ligands show high affinity. Nevertheless, polypharmacology is considered an appropriate solution to achieve high-efficacy complex therapy for mood disorders and schizophrenia. Some new trends in searching against the most common central nervous system disorders indicate the importance of serotonin and dopamine target, besides 5-HT_7, 5-HT_{1A}, and D_2 receptors. However, different studies demonstrate various dual- and multitarget acting compounds that are useful against CNS disorders, which involve serotoninergic receptors and other GPCRs, like muscarinic M4 receptors against schizophrenia.[8]

Among different studies,[9–17] performed in our laboratories, that led to the synthesis of serotoninergic ligands characterized by high affinity and selectivity, we described the synthesis and pharmacological evaluation of a set of derivatives where the piperazine-*N*-alkyl moiety has been linked via 2-hydroxypropyl spacing unit to norbornene and *exo*-*N*-hydroxy-7-oxabicyclo[2.2.1]hept-5-ene-2,3-dicarboximide nuclei, respectively; the binding data reported in these studies evidenced as the combination of these structural elements afforded compounds with an interesting affinity/selectivity profile toward 5-HT_{1A} and 5-HT_{2C} receptors.[18] These results prompted us, in continuation of our research program, to complete the norbornene and *exo*-*N*-hydroxy-7-oxabicyclo[2.2.1]hept-5-ene-2,3-dicarboximide series with some arylpiperazines that had not been considered previously (Tables 1 and 2). All the new compounds were tested for their functional activity or affinity to 5-HT_{1A}, 5-HT_{2A}, and 5-HT_{2C} receptors, and their multireceptor profiles were also evaluated in terms of functional activity for dopaminergic (D_2) and muscarinic receptors. Moreover, compounds showing the best affinity and selectivity binding profiles toward serotoninergic receptors, including also compounds belonging to the previously synthetized series, have been evaluated by in vivo assay (i.e., behavioral tests), with the aim to discover novel pharmacological tools useful in treating psychiatric and neurological disorders, such as schizophrenia, depression, and anxiety. Therefore, we evaluated antipsychotic activity of the compounds in amphetamine-induced hyperactivity test, antidepressant-like activity in the forced swim test (FST), and anxiolytic-like effects in the elevated plus-maze test (EPM). Moreover, we used additional tests—spontaneous locomotor activity, rotarod, chimney test, and bar test—to assess potential adverse effects of the compounds. Results obtained from the tested compounds in the FST were compared with commonly known antidepressant, fluoxetine, and those in EPM with the clinically useful anxiolytic, buspirone.

2 | RESULTS AND DISCUSSION

2.1 | Chemistry

The general strategy for the synthesis of the target compounds (Tables 1 and 2) is summarized in Scheme 1. The general procedure is as follows: alkylation of the starting 4-X-substituted piperazines with epichlorohydrin in absolute ethanol gave the corresponding 3-chloro-2-hydroxypropyl-4-X-substituted piperazines **2f–n**. The obtained intermediates were condensed with the desired heterocycle *endo*-*N*-hydroxy-5-norbornene-2,3-dicarboximide or *exo*-*N*-

TABLE 1 Agonist activity of compounds **3f**–**n** at the 5-HT_{1A} receptor

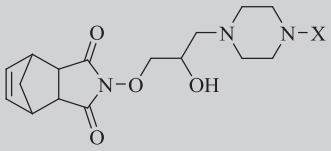

Compound[a]	X	5-HT_{1A} receptor G-protein stimulation		
		pEC_{50}	EC_{50} ± *SEM* (nM)	E_{max} ± *SEM* (%)
3f	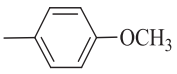	No activity	No activity	No activity
3g	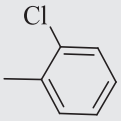	5.9 ± 0.44	1266 ± 275	122.4 ± 6.3*
3h	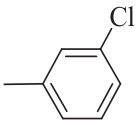	No activity	No activity	No activity
3i	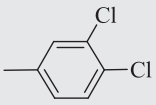	No activity	No activity	No activity
3j	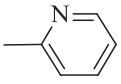	4.3 ± 0.4	41360 ± 2510	122 ± 8.75*
3k	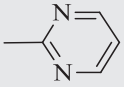	No activity	No activity	No activity
3l	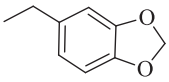	No activity	No activity	No activity
3m	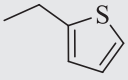	No activity	No activity	No activity
3n	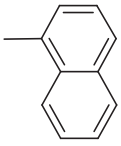	No activity	No activity	No activity
8-OH-DPAT		7.5 ± 0.11	27.2 ± 0.13	154 ± 2.3

[a]All the final compounds have been obtained and tested as racemic mixtures (*R*,*S*); [α]25D = ±0.01° (*c* = 0.01, MeOH).

*$p < .01$ versus 8-OH-DPAT.

hydroxy-7-oxabicyclo[2.2.1]hept-5-ene-2,3-dicarboximide, in the presence of NaOH pellets in absolute ethanol, to give the final compounds **3f**–**n** and **4f**–**n**. Purification of each final product was carried out by chromatography on silica gel column and further by crystallization from the appropriate solvent. All new compounds gave satisfactory elemental analysis results, and they were characterized by ^{1}H NMR and mass spectrometry (API 2000 Applied Biosystem). ^{1}H nuclear magnetic resonance (NMR), mass spectrometry (MS), and optical data for all final compounds obtained as racemic mixtures were consistent with the proposed structures.

2.2 | Pharmacology

2.2.1 | Agonistic and antagonistic activity against the 5-HT_{1A} receptor: Functional studies

Four newly synthesized arylpiperazines demonstrated an agonistic activity at the 5-HT_{1A} receptor (Tables 3 and 4). Basal 5-HT_{1A} stimulation was set to 100%. When 2-chlorophenylpiperazines derivatives (**3g**, **4g**) were compared, they both expressed similar efficacies and equally low potencies. The E_{max} (baseline G-protein

TABLE 2 Agonist activity of compounds **4f**–**n** at the 5-HT_{1A} receptor

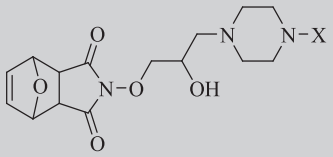

	5-HT_{1A} receptor G-protein stimulation			
Compound[a]	X	pEC_{50}	EC_{50} ± *SEM* (nM)	E_{max} ± *SEM* (%)
4f	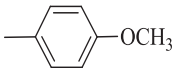	No activity	No activity	No activity
4g	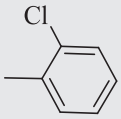	5.8 ± 0.36	1388 ± 229	138.6 ± 10
4h	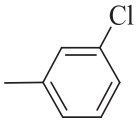	No activity	No activity	No activity
4i	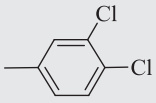	No activity	No activity	No activity
4j	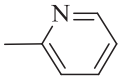	6.4 ± 0.4*	327.7 ± 26.9	128 ± 5.4**
4k	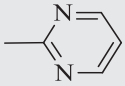	No activity	No activity	No activity
4l	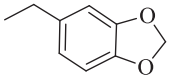	No activity	No activity	No activity
4m	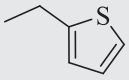	No activity	No activity	No activity
4n	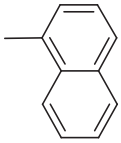	No activity	No activity	No activity
8-OH-DPAT		7.5 ± 0.11	27.2 ± 0.13	154 ± 2.3

[a]All the final compounds have been obtained and tested as racemic mixtures (*R*,*S*); [α]25D = ±0.01° (*c* = 0.01, MeOH).

*$p < .05$ versus **4j**.

**$p < .01$ versus 8-OH-DPAT.

stimulation was set to 100%) value for compound **3g** classified it as a partial agonist (122.4% ± 6.3%), with potency (pEC_{50}) equaling 5.9 ± 0.44, whereas the corresponding values for its analog (**4g**) were 138.6% ± 10% and 5.8 ± 0.36, respectively. Thus, the heterocyclic scaffold does not influence pEC_{50} ($F_{1,36} = 0.92$; $p > .05$) or E_{max} ($F_{1,36} = 1.4$; $p > .05$) parameters of the compound. In contrast, the pyridyl piperazine derivative supporting an *exo*-*N*-hydroxy-7-oxabicyclo[2.2.1]hept-5-ene-2,3-dicarboximide scaffold as a terminal fragment (**4j**) was more potent ($pEC_{50} = 6.4 \pm 0.4$) than its analog (**3j**; $pEC_{50} = 4.3 \pm 0.4$; $F_{1,36} = 4.7$; $p < .05$). On the contrary, both compounds expressed a comparable partial agonist activity (128% ± 5.4% and 122% ± 8.75%; $F_{1,36} = 0.8$; $p > .05$). Instead, both 4-methoxyphenylpiperazine derivatives (**3f** and **4f**), the norbornene derivative supporting a 3-chlorophenylpiperazine moiety (**3h**), and the derivative containing a naphthylpiperazine moiety (**4n**) acted as antagonists at the 5-HT_{1A} receptor. In particular, the strongest antagonistic profile was observed for **4n** ($pIC_{50} = 6.8 \pm 0.15$; $F_{4,85} = 26.3$; $p < .001$).

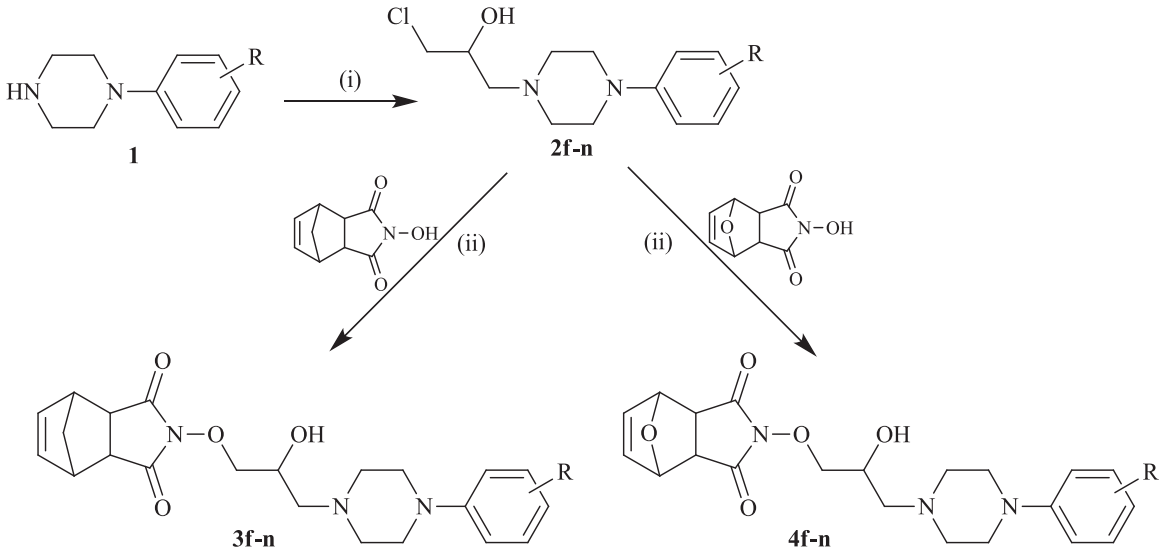

SCHEME 1 Reagents and conditions: (i) Cl–CH_2–CH(O)CH_2, EtOH abs; (ii) NaOH pellets, EtOH abs

2.2.2 | Binding affinity to the 5-HT_{2A} and 5-HT_{2C} receptors: Competition studies

All the new compounds were tested for their affinity to 5-HT_{2A} and 5-HT_{2C} receptors. Some of the newly synthesized derivatives showed interesting affinity values in the nanomolar range toward 5-HT_{2A} receptors and lower affinity toward 5-HT_{2C} receptors (Tables 5 and 6). Besides the outstanding 5-HT_{2A} receptor affinity and selectivity of compounds **3i** (K_i = 32.7 nM with pK_i = 7.48 ± 0.05 [$F_{1,38}$ = 182.8; p < .001]) and **3n** (K_i = 80 nM with pK_i = 7.1 ± 0.06 [$F_{1,38}$ = 36.7; p < .001]), other interesting K_i values were those of compounds **3h** (K_i = 371 nM with pK_i = 6.4 ± 0.086 [$F_{1,38}$ = 41.1; p < .001]), **4n** (K_i = 465 nM with pK_i = 6.3 ± 0.097), **4i** (K_i = 542 nM with pK_i = 6.2 ± 0.058), and **3g** (K_i = 699 nM with pK_i = 6.16 ± 0.11 [$F_{1,38}$ = 22.1; p < .001]). Moreover, compound **3n** showed an interesting mixed 5-HT_{2A}/5-HT_{2C} profile with K_i values of 80/92.9 nM, whereas compounds **4n**, **3n**, and **4l** presented the most attractive 5-HT_{2C} affinity profile with K_i values of 69, 92.9, and 429 nM and pK_i values of 7.1 ± 0.16, 7.03 ± 0.15, and 6.37 ± 0.14, respectively.

As compared with the reference 5-HT_{2A} receptor ligand, ketanserin (pK_i = 8.27 ± 0.06), one can conclude that compounds **3i**, **3n**, **3h**, **4n**, **4i**, and **3g** expressed satisfactory affinities to the 5-HT_{2A} receptor. Simultaneously, the 3,4-dichloro-, naphthyl-, 3-chloro- and 2-chlorophenylpiperazine substituents had the strongest influence on the 5-HT_{2A} receptor binding affinity. When comparing the evaluated series of arylpiperazine derivatives with 5-HT_{2C} receptor-selective ligands, such as RS-102221 (pK_i = 8.34 ± 0.12), one can point out 2-hydroxypropoxyl derivatives supporting the naphthylpiperazine moiety as a terminal group (**3n** and **4n**) as the most promising, with their pK_i value below 100 nM. The class of moderate affinity 5-HT_{2C} receptor ligands (pK_i lower than 1 μM) consisted of piperonylpiperazines (**3l** and **4l**) and 3,4-dichlorophenylpiperazine (**3i** and **4i**) derivatives. Finally, none of the tested compounds expressed an antagonistic activity against the D_2 receptor.

The difference in affinity observed between this new series of derivatives (**3f**–**n** and **4f**–**n**) and the previously described series,[18] characterized by the same norbornene or analog *exo*-*N*-hydroxy-7-oxabicyclo[2.2.1]hept-5-ene-2,3-dicarboximide nucleus linked via 2-hydroxypropyl spacing unit to 4-substituted piperazines, further demonstrates that the isosteric substitution of a methylene group (**3f**–**n**) with an oxygen atom (**4f**–**n**) does not represent a critical feature in determining differences in binding with 5-HTRs. Once again, also in these novel derivatives, although they have a lower affinity profile than the previously synthesized derivatives, the influence of the 2-hydroxypropyl spacer associated with the appropriate substituents on the phenylpiperazine ring and heterocyclic nucleus was particularly profitable, not only in relation to 5-HT_{1A} functional activity, but also 5-HT_{2A} and 5-HT_{2C} receptor affinity. However, to rationalize the differential binding affinities/activities, molecular docking studies were carried out on the complete series of derivatives.

2.2.3 | In vitro evaluation of 5-HT-evoked contractions

Successively, compounds **3n** and **3i** with better affinity/selectivity binding profiles toward 5-HT_{2A} receptors have been tested by in vitro assay to determine their activity concerning 5-HT-evoked contractions. In the rat ileum, 5-HT_{2A} receptors are located on smooth muscles and their activation by 5-HT is known to induce contraction. Consequently, 5-HT_{2A} antagonists depress 5-HT-induced contractions in the rat ileum.[19] According to Briejer and colleagues, we have shown that 5-HT contracted the rat ileum longitudinal muscle. In preliminary experiments, we found that the neuronal blocker tetrodotoxin

TABLE 3 Antagonistic activity of compounds **3f–n** at the 5-HT_{1A} receptor

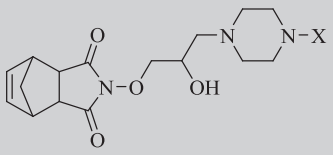

	5-HT_{1A} receptor G-protein stimulation			
Compound[a]	X	pIC_{50} ± *SEM*	IC_{50} ± *SEM* (nM)	pK_B ± *SEM*
3f	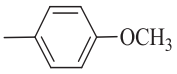	4.5 ± 0.19	29890 ± 1458	4.95 ± 0.16
3g	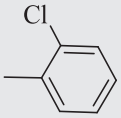	No activity	No activity	No activity
3h	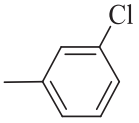	4.6 ± 0.4	26090 ± 2511	4.96 ± 0.3
3i	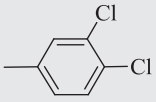	No activity	No activity	No activity
3j	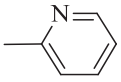	No activity	No activity	No activity
3k	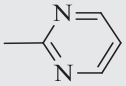	No activity	No activity	No activity
3l	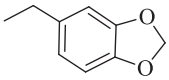	No activity	No activity	No activity
3m	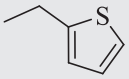	No activity	No activity	No activity
3n	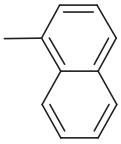	No activity	No activity	No activity
WAY-100635		8.4 ± 0.12	4.3 ± 1.4	8.78 ± 0.15

[a]All the final compounds have been obtained and tested as racemic mixtures (*R*,*S*); [α]25D = ±0.01° (*c* = 0.01, MeOH).

(0.3 μM), the muscarinic receptor antagonist atropine (1 μM), the adrenergic receptor antagonist phentolamine (10−6 M) plus propranolol (10−6 M) did not affect the contractions by 5-HT. In contrast, ketanserin (0.1 μM), at a concentration that blocks 5-HT_{2A} receptors, depressed the contractions induced by 5-HT. Collectively, these results suggest that 5-HT contracts the ileum by acting on 5-HT_{2A} receptors located on smooth muscle, whereas muscarinic or adrenergic receptors are not involved. Results show the potency (expressed by the IC_{50} value) and the efficacy (expressed by the E_{max} value) of the compounds under investigation in inhibiting 5-HT-induced contractions in the rat ileum (a pharmacological assay useful to detect activity toward 5-HT_{2A} receptors). The compounds under investigation, **3n** (E_{max} = 26.66%) and **3i** (E_{max} = 16.87%), did not significantly inhibit the contractions induced by 5-HT. The rank order of efficacy was **3n** > **3i**. Concerning the potency, these compounds displayed potency approximately in the 10^{-6} to 10^{-5} M range; specifically, the rank order of potency was **3n** (1.08×10^{-6} M) > **3i** (1.05×10^{-5} M). Finally, none of the compounds under investigation contracted, per se, the rat ileum.

TABLE 4 Antagonistic activity of compounds **4f–n** at the 5-HT_{1A} receptor

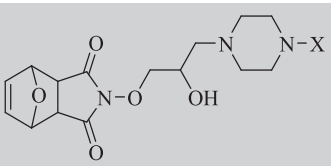

		5-HT_{1A} receptor G-protein stimulation		
Compound[a]	X	pIC_{50} ± *SEM*	IC_{50} ± *SEM* (nM)	pK_B ± *SEM*
4f	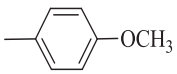	4.7 ± 0.2	21310 ± 1584	5.05 ± 0.3
4g	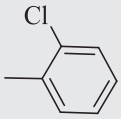	No activity	No activity	No activity
4h	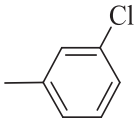	No activity	No activity	No activity
4i	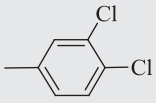	No activity	No activity	No activity
4j	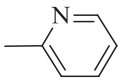	No activity	No activity	No activity
4k	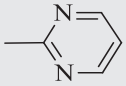	No activity	No activity	No activity
4l	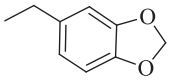	No activity	No activity	No activity
4m	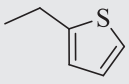	No activity	No activity	No activity
4n	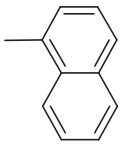	6.8 ± 0.15	129.7 ± 14.9	7.56 ± 0.19
WAY-100635		8.4 ± 0.12	4.3 ± 1.4	8.78 ± 0.15

[a]All the final compounds have been obtained and tested as racemic mixtures (*R*,*S*); [α]25D = ±0.01° (*c* = 0.01, MeOH).

2.3 | Molecular docking studies

The analysis of molecular docking results of compounds **3f–n** and **4f–n**, including also compounds previously synthetized (**3a–e** and **4a–e**; Figure 1),[18] with all the studied receptors indicated that, in general, the docking scores were comparable for both enantiomers. Slightly higher values were obtained for *R* enantiomers, so the receptor complexes with *R* enantiomers were used for further analysis. Figures 2–4 present the results of molecular docking of selected compounds to serotonin 5-HT_{1A}, 5-HT_{2A}, and 5-HT_{2C} receptors, respectively. The rationale for compound selection for the detailed description of molecular ligand–receptor interactions was (i) their best receptor affinity at each receptor and (ii) selection of the compound for in vivo studies. As the studied ligands follow the classical pharmacophore model for aminergic GPCR ligands,[20] the electrostatic interaction between their protonatable nitrogen atoms and Asp3.32 is their main contact with the receptors.[21] In the case of all receptors and most active ligands, Trp6.46 and Phe6.52 are residues involved in π–π stacking interactions with *N*-aryl groups of the compounds, as reported previously for many similar ligand–receptor complexes.[22–26] Such a pattern of ligand–receptor interactions was

TABLE 5 Affinities of compounds **3f–n** toward the 5-HT_{2A} and 5-HT_{2C} receptors

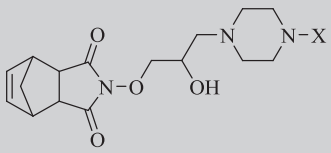

Compound[a]	X	Receptor binding affinity 5-HT_{2A} pK_i	5-HT_{2A} $K_i \pm SD$ (nM)	5-HT_{2C} pK_i	5-HT_{2C} $K_i \pm SD$ (nM)
3f	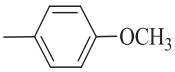	5.16 ± 0.07	6880 ± 1186	5.09 ± 0.14	7995 ± 403
3g	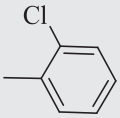	6.16 ± 0.11	699 ± 126	5.57 ± 0.25	2635 ± 1380
3h	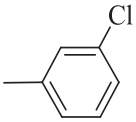	6.4 ± 0.086	371 ± 122	4.99 ± 0.13	10080 ± 7413
3i	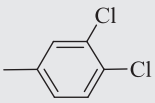	7.48 ± 0.05	32.7 ± 11.2	6.21 ± 0.15	609 ± 142
3j	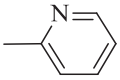	5.2 ± 0.045	5508 ± 1109	5.26 ± 0.26	5438 ± 1819
3k	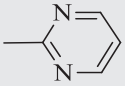	4.96 ± 0.11	10920 ± 5959	5.3 ± 0.19	4767 ± 646
3l	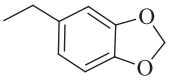	4.2 ± 0.17	56560 ± 14791	6.26 ± 0.14	544 ± 266
3m	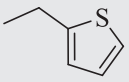	5.9 ± 0.32	1034 ± 209	5.8 ± 0.31	1482 ± 204.2
3n	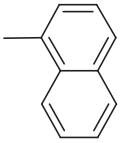	7.1 ± 0.06	80 ± 11.6	7.03 ± 0.15	92.9 ± 4.7
Ketanserin		8.27 ± 0.06	5.3 ± 1.12		
RS-102221				8.34 ± 0.12	4.51 ± 0.17
Serotonin				8.14 ± 0.15	7.17 ± 3.5

[a]All the final compounds have been obtained and tested as racemic mixtures (*R*,*S*); [α]25D = ±0.01° (*c* = 0.01, MeOH).

found for ritanserin, an inverse agonist of serotonin 5-HT_{2C} receptor, in the X-ray structure of the respective ligand–receptor complex (PDB ID: 6BQH[27]). This binding pose was verified by mutation of Phe5.47, Phe6.44, and Trp6.48. Moreover, residues from extracellular loop 2 (ecl2) are also important for ligand–receptor interactions, and they may be responsible for subtype-selective interactions,[28,29] as they constitute a differentiated receptor part involved in the recognition of the "address" part of the ligands.[30]

The ligands adopt an expanded docking conformation and are situated parallel to the transmembrane helices. Their norbornene or *exo*-*N*-hydroxy-7-oxabicyclo[2.2.1]hept-5-ene-2,3-dicarboximide moiety is directed toward the extracellular vestibule, whereas their *N*-aryl group penetrates deeper into the cavities of the receptors, which is also in accordance with the binding pose of ritanserin in its abovementioned complex with serotonin 5-HT_{2C} receptor resolved by X-ray crystallography. The affinity of the studied compounds to

TABLE 6 Affinities of compounds **4f–n** for 5-HT_{2A} and 5-HT_{2C} receptors

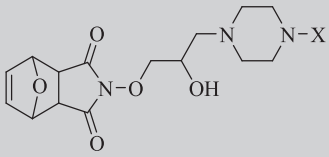

Compound[a]	Receptor binding affinity X	5-HT_{2A} pK_i	5-HT_{2A} $K_i \pm SD$ (nM)	5-HT_{2C} pK_i	5-HT_{2C} $K_i \pm SD$ (nM)
4f	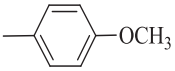	4.5 ± 0.07	29070 ± 11906	4.2 ± 0.38	58830 ± 24417
4g	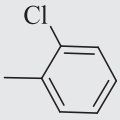	5.3 ± 0.098	5955 ± 1253	4.7 ± 0.21	17580 ± 6115
4h	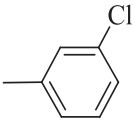	5.65 ± 0.074	2220 ± 210	5.67 ± 0.13	2094 ± 134
4i	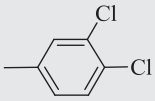	6.2 ± 0.058	542 ± 114	6.15 ± 0.10	708 ± 235
4j	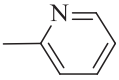	5.5 ± 0.11	2812 ± 1288	4.74 ± 0.18	17960 ± 6606
4k	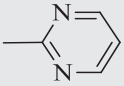	4.5 ± 0.1	28630 ± 13098	5.1 ± 0.14	7626 ± 323
4l	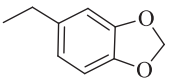	4.5 ± 0.13	31230 ± 13489	6.37 ± 0.14	429 ± 112
4m	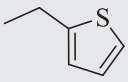	5.8 ± 0.25	1625 ± 678	4.9 ± 0.4	11010 ± 2512
4n	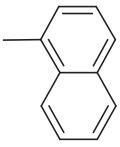	6.3 ± 0.097	465 ± 125	7.1 ± 0.16	69.9 ± 14.4
Ketanserin		8.27 ± 0.06	5.3 ± 1.12		
RS-102221				8.34 ± 0.12	4.51 ± 0.17
Serotonin				8.14 ± 0.15	7.17 ± 3.5

[a]All the final compounds have been obtained and tested as racemic mixtures (*R*,*S*); [α]25D = ±0.01° (*c* = 0.01, MeOH).

serotonin receptor subtypes is mainly affected by the type of *N*-aryl substituents, and it is, to the lesser extent, driven by the presence of norbornene or *exo*-*N*-hydroxy-7-oxabicyclo[2.2.1]hept-5-ene-2,3-dicarboximide moiety, as previously reported by Zagórska et al.[31] for similar molecules. Following their results, *ortho*, *meta*, or *para* substitutions on the phenyl ring seem to be generally preferred over *para* substitution. This can be a consequence of the favorable pattern of hydrogen bond interactions with *ortho*-methoxy group (compounds **3a** and **4a**) and/or most advantageous positions *ortho*- and *meta*-substituted compounds can adopt in the binding site (compounds **3b**, **3d**, **3g**, **3h**, **4b**, **4d**, **4g**, and **4h**). Good affinity of compounds **3g**, **3h**, **3i**, and **4i** to serotonin 5-HT_{2A} receptor may be explained by the possibility of halogen bond formation, as suggested by Partyka et al.[32]

Concerning serotonin receptor subtype selectivity of the investigated molecules, for the interactions of arylpiperazine group

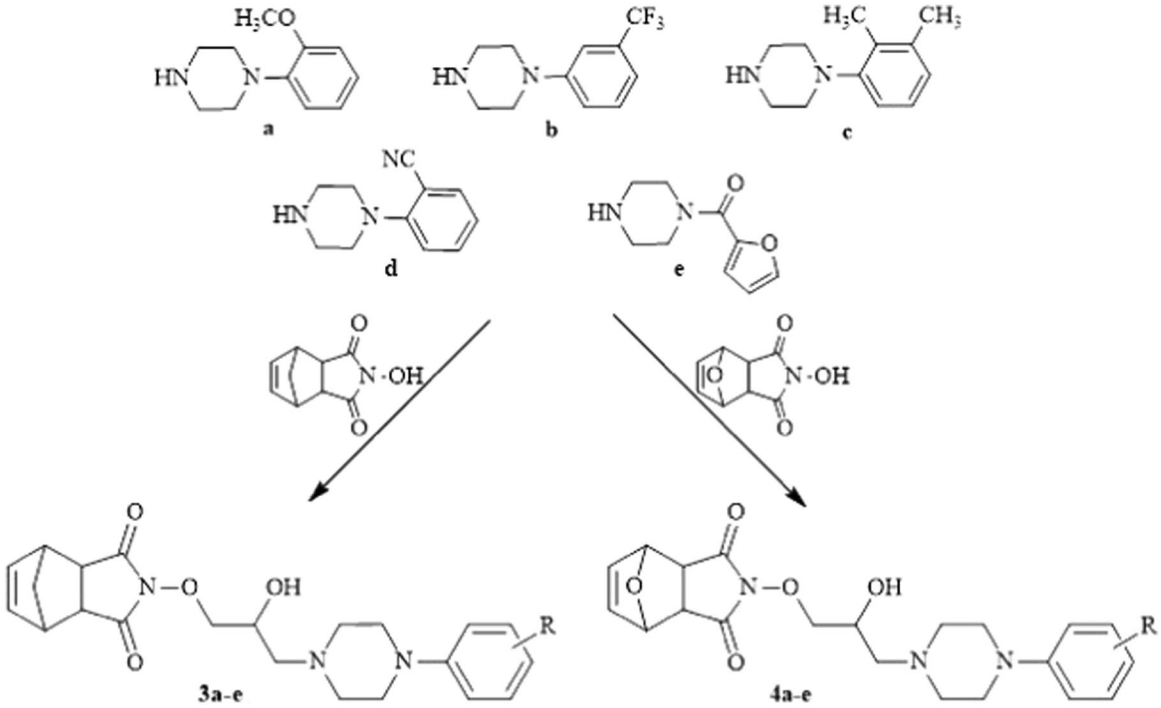

FIGURE 1 Norbornene and *exo-N*-hydroxy-7-oxabicyclo[2.2.1]hept-5-ene-2,3-dicarboximide series (**3a**–**e** and **4a**–**e**) previously synthesized

with serotonin 5-HT_2 receptor subtypes, Asp3.32, Trp6.48, and one or more aromatic residues at positions 5.47 and/or 6.52 are required. For the serotonin 5-HT_{2A} receptor, Trp7.39 can be also important.[33] Our earlier molecular modeling studies allowed to conclude that for the interactions with serotonin 5-HT_{2C} receptor, the ligands may form additional hydrogen bonds with Ser2.60 or Asn7.35, which are not found for interactions with 5-HT_{1A} and 5-HT_{2A} receptors.[34] In contrast, here we observed that Asn7.38 and Tyr7.42 seem to be crucial for interactions with serotonin 5-HT_{1A} receptor. As an example, when the selectivity profile of compound **3n** versus **4n** is compared, the better affinity of compound **3n** to 5-HT_{2A} receptor can result from additional π–π stacking interaction with Phe6.51; however, both ligands interact with Asp3.32, Trp6.48, and Phe6.52. In the case of 5-HT_{2C} receptor, the affinity of both compounds is comparable and results from interactions with Asp3.32, Phe5.47, Trp6.48, and Phe6.52.

To study how a nonselective or a multitarget ligand **4n** fits to the binding pocket of all receptors, noncovalent interaction (NCI) maps were generated. In the case of all receptors, compound **4n** fits well to the binding cavities, as depicted in Figure 5a–c. NCI is a visualization index derived from the density and identification of NCIs. It is based on the peaks that appear in the reduced density gradient at low densities.[35a] To further describe interactions of compound **4n** with the studied receptors, the most important ligand–receptor contacts are shown in Table 7. It can be seen that π–π stacking interactions between side chains of aromatic residues (in particular Trp6.48 and Phe6.52) and the ligand naphthyl moiety are an important contribution to interaction energy, as reported earlier.[35b,c] Better affinity of compound **4n** to serotonin 5-HT_{2C} receptor versus 5-HT_{2A} receptor can be attributed to the greater number of aromatic interactions and additional hydrogen bond with Tyr7.42.

In conclusion, the molecular modeling results described above may be useful to design serotonin receptor ligands with required selectivity or polypharmacology.

2.4 | In vivo behavioral tests

Compounds **3b**, **3e**, and **4a** from the previously published series and compounds **4j** and **4n** from this study were selected for further functional in vivo studies. The first part of the experiments included locomotor activity and motor coordination tests, generally accepted as basic in central activity investigations of new agents.[36] First, none of the compounds at the dose of 30 mg/kg changed the behavior of mice in the chimney test (Figure 6a) and impaired motor coordination assessed in the rotarod test (Figure 6b). In the locomotor activity test, only compound **4j** at a dose of 30 mg/kg decreased the spontaneous motility after 6 min (Figure 7a) and 20 min (Figure 7b) of observation.

In the second stage of this study, we evaluated the antipsychotic ability of the new compounds. Animal models of schizophrenia, commonly employed for preclinical studies of antipsychotic properties of drugs, consider mainly amphetamine and MK-801 models.[37] The first model is based on the manipulation of the dopaminergic system, and it may primarily respond to drugs that affect this neurotransmitter system. Many neuroleptics acting as dopaminergic antagonists reverse this effect.[38] It is noteworthy that amphetamine-induced hyperlocomotion is sensitive to other classes of drugs, including mGluR2/3 agonists.[39]

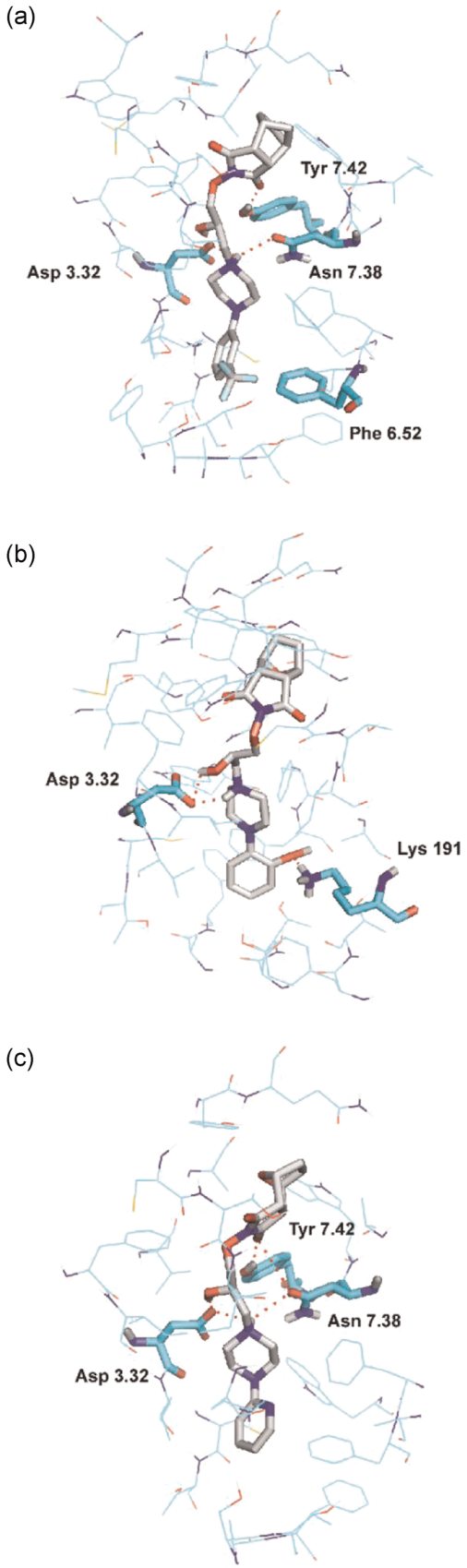

On the contrary, several preclinical tests have pointed to the role of 5-HT_{2C} ligands in the modulation of monoaminergic systems, including dopaminergic. Indeed, dysfunction in serotoninergic activity could contribute to the alteration of dopaminergic function seen in schizophrenia.[40] In the amphetamine model, all tested compounds at a dose of 15 mg/kg reduced amphetamine-induced hyperactivity of mice (Figure 8). The observed positive antipsychotic effect could be related rather to their interaction with other than dopaminergic receptors, because the compounds evaluated are weak ligands of D_1 and D_2 receptors. However, 5-HT_{2C} and/or 5-HT_{1A} receptors, through modulation of the dopaminergic system, may play a significant role in this activity.

Another animal model used in this type of research is the MK-801-induced hyperactivity test. Apart from the dopaminergic hypothesis, numerous data also indicate the role of the glutamatergic system in the development of schizophrenia. *N*-Methyl-D-aspartate (NMDA) receptor ligands, for example, MK-801, with antagonistic properties, increase locomotor activity and disturb memory processes.[41] Only compound **3e**, used at the dose of 15 mg/kg, reduced the increased locomotor activity of the animals in this test, which indicates that its mechanism of action may be related to NMDA receptors (Figure 9).

Furthermore, due to the modulation of the central serotonin neurotransmission, the new compounds may also show an anxiolytic and/or antidepressant activity.[42,43] Considering this premise, as well as in vitro data obtained for the test compounds (mixed 5-HT_{1A}/5-HT_{2C} affinity profile for all the compounds), we examined their antidepressant and anxiolytic potential in behavioral models commonly used in mice, that is, FST and EPM.

The obtained results indicated that, except for **4j**, all the tested compounds (15 and 30 mg/kg) revealed antidepressant-like properties, observed as a shortening of the immobility time of mice to various extents in the FST (Figure 10). In addition, fluoxetine at the dose of 15 mg/kg, used as a reference drug, caused a statistically significant decrease in immobility time. Interestingly, compound **4j** and two compounds active in the FST test (**3e** and **4n**) exhibited characteristics of anxiolytic drugs: They increased in a statistically significant manner the percentage of entries and the time spent in the open arms of the EPM. Compounds **3b** and **4a** were inactive. This test is based on the hypothesis that exposure to an elevated and open maze alley leads to an approach–avoidance conflict that is considerably stronger in comparison to that evoked by exposure to a closed maze alley.[44] Fear-induced inhibition of exploratory activity affects entries into open arms in this task. As a

FIGURE 2 Selected ligands in complex with serotonin 5-HT_{1A} receptor: (a) **3b**, (b) **4a**, and (c) **4j**. Proteins are shown in wire representation with cyan carbon atoms. The most important residues are shown as sticks. Ligands are shown as sticks with gray carbon atoms. Polar interactions are shown as red dashed lines. Nonpolar hydrogen atoms are omitted for clarity

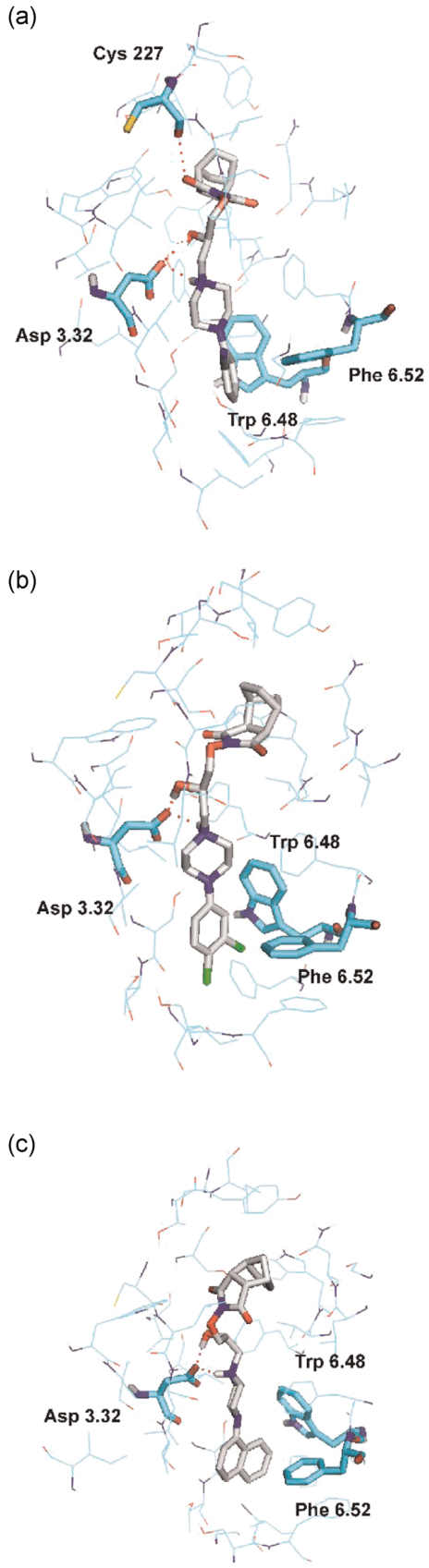

significant increase in the percentage of time spent on the open arms and the number of entries into open arms is observed only with drugs that are clinically effective anxiolytics,[45] this model has been used to assess anxiolytic-like activity of new putative anxiolytic compounds.[46] Buspirone (5 mg/kg) used as a reference anxiolytic drug also prolonged time and increased the percentage of entries into the open arms (Figure 11). In this test, the new compounds **3e**, **4j**, and **4n** were comparably efficacious to buspirone.

In addition, we evaluated the potential adverse effects of the compounds as the risk of catalepsy in the bar test. The motor side effects of antipsychotic drugs are a main concern in clinics. Therefore, various behavioral tests have been developed to determine whether new antipsychotic agents or strategies generate motor side effects in comparison to classical antipsychotics. Catalepsy in the bar test is a frequently used model to predict the liability of drugs to produce extrapyramidal side effects in humans.[47] By themselves, 5-HT_{2C} ligands do not induce catalepsy.[48] Accordingly, any of the here reported compounds exert cataleptogenic effects in the bar test.

In schizophrenia, there are additional cognitive disturbances in the form of memory dysfunction, decreased concentration, or a decrease in IQ. 5-HT_{1A} receptors play an important role in these processes.[49] The effect of the new compounds on memory impairment was assessed in the passive avoidance (PA) test, which exploits the considerable preference of rodents for darkened versus illuminated places. An additional aversive stimulus is an electrical impulse in the darkened zone. Memory deficit in an animal model of cognitive impairment was caused by the administration of MK-801 at a dose of 0.3 mg/kg. The tested compounds **3e**, **4j**, and **4n**, used at the dose of 15 mg/kg, significantly improved memory in mice treated with MK-801 (Figure 12). The measure of this activity was the lengthening of the transition time to the dark room, compared with the control group and, at the same time, the increase of the latency index (LI). Thus, these compounds clearly compensate for memory deficits and stimulate consolidation processes. These results may indicate the association of the activity of **3e**, **4j**, and **4n** with their affinity for the 5-HT_{1A} receptor.[50,51]

3 | CONCLUSIONS

We have described the synthesis of a new series of arylpiperazines as serotoninergic ligands (**3f–n** and **4f–n**). The pyridyl piperazine derivative supporting an *exo*-*N*-hydroxy-7-oxabicyclo[2.2.1]hept-5-

FIGURE 3 Selected ligands in complex with serotonin 5-HT_{2A} receptor: (a) **3d**, (b) **3i**, and (c) **3n**. Proteins are shown in wire representation with cyan carbon atoms. The most important residues are shown as sticks. Ligands are shown as sticks with gray carbon atoms. Polar interactions are shown as red dashed lines. Nonpolar hydrogen atoms are omitted for clarity

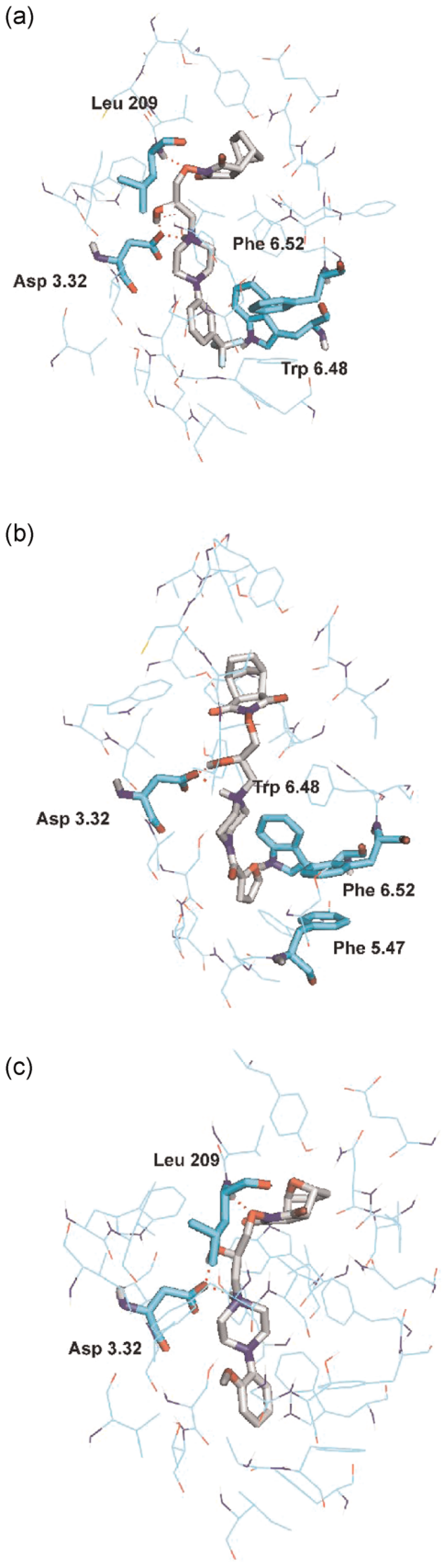

ene-2,3-dicarboximide scaffold as a terminal fragment (**4j**) afforded a favorable agonistic profile for 5-HT_{1A} receptors (pEC_{50} = 6.4 ± 0.4), whereas the derivative containing a naphthylpiperazine moiety (**4n**) showed an interesting antagonist profile at the 5-HT_{1A} receptor (pEC_{50} = 6.8 ± 0.15). Due to their high potency at the 5-HT_{1A} receptor affinity and selectivity, these compounds were selected together with compounds **3b**, **3e**, and **4a** from the previously published series for further in vivo studies to investigate their functional activity.

The obtained results showed that, except for **4j**, all tested compounds exerted antidepressant-like effects. Interestingly, compounds **3n**, **4j**, and **4n** revealed significant anxiolytic properties and, in the EPM test, they were almost as efficacious as buspirone. Additionally, no side effects, like catalepsy and motor impairment, were observed after the injection of the tested compounds. Finally, the derivatives **3e**, **4j**, and **4n** showed a marked improvement of memory in mice treated with MK-801, indicating the association of activity of these compounds with their affinity for the 5-HT_{1A} receptor.[50,51] However, further pharmacological studies are necessary to determine their detailed mechanism of action and prospective clinical usefulness.

In conclusion, data presented in this study confirm that, as obtained with the series previously synthesized,[21,22] the novel synthesized compounds display a general trend of affinity toward 5-HT_{1A} receptors. Molecular docking studies supported these results, highlighting some selective and additional interactions of the identified ligands with the investigated receptor subtype.

4 | EXPERIMENTAL

4.1 | Chemistry

4.1.1 | General

All reagents and substituted piperazines were commercial products purchased from Sigma-Aldrich. Melting points, determined using a Buchi Melting Point B-540 instrument, are uncorrected and represent values obtained on recrystallized or chromatographically purified material. ^{1}H NMR spectra were recorded on a Varian Mercury Plus 400 MHz instrument. Unless otherwise stated, all spectra were recorded in $CDCl_3$. Chemical shifts are

FIGURE 4 Selected ligands in complex with serotonin 5-HT_{2C} receptor: (a) **3b**, (b) **3e**, and (c) **4a**. Proteins are shown in wire representation with cyan carbon atoms. The most important residues are shown as sticks. Ligands are shown as sticks with gray carbon atoms. Polar interactions are shown as red dashed lines. Nonpolar hydrogen atoms are omitted for clarity

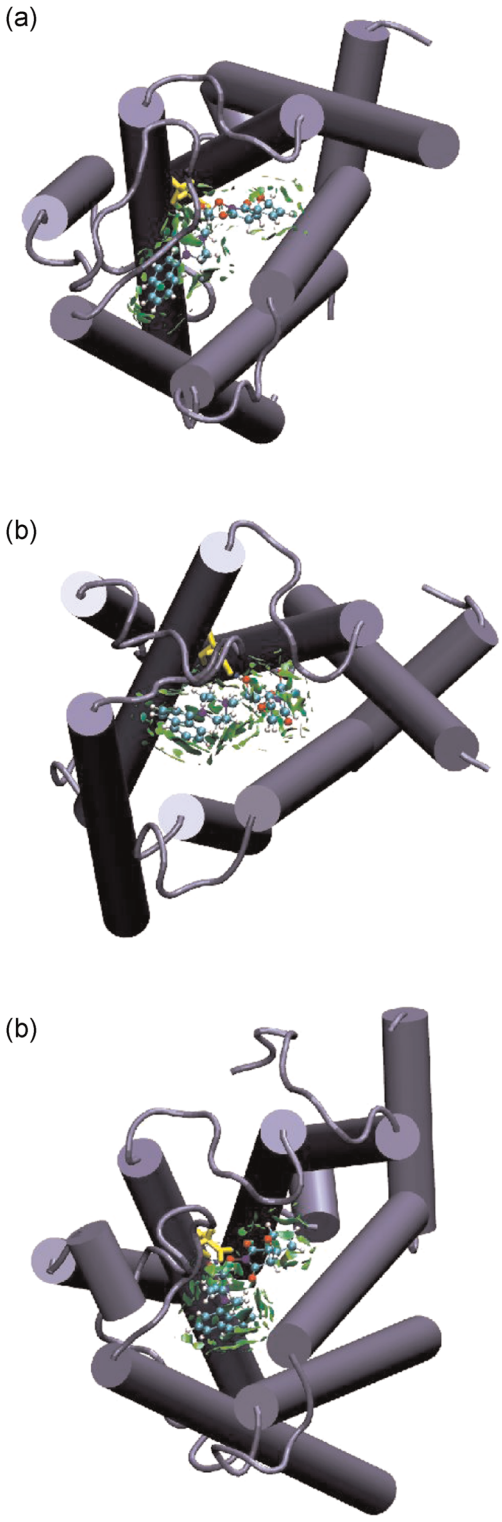

FIGURE 5 Noncovalent interaction maps for compound **4n** in complex with serotonin (a) 5-HT_{1A}, (b) 5-HT_{2A}, and (c) 5-HT_{2C} receptors. Weak attractive interactions are shown in green. Proteins are shown in ice-blue as cartoon representation. Asp3.32 is shown in yellow in stick representation. Compound **4n** is shown in Corey–Pauling–Koltun representation with cyan carbon atoms

TABLE 7 Molecular interactions of nonselective compound **4n** with serotonin 5-HT_{1A}, 5-HT_{2A}, and 5-HT_{2c} receptors

$5HT_{1A}$ receptor	5-HT_{2A} receptor	5-HT_{2C} receptor
Asp3.32 salt bridge	Asp3.32 salt bridge	Asp3.32 salt bridge
Tyr7.42 hydrogen bond	Trp6.48 π–π stacking	Tyr7.42 hydrogen bond
Phe6.52 π–π stacking	Phe6.52 π–π stacking	Phe5.47 π–π stacking
		Trp6.48 π–π stacking
		Phe6.52 π–π stacking

reported in ppm. The following abbreviations are used to describe peak patterns when appropriate: s (singlet), d (doublet), t (triplet), m (multiplet), q (quartet), qt (quintet), dd (doublet of doublet), bs (broad singlet), and mm (multiplet of multiplet). Mass spectra of the final products were recorded on an API 2000 Applied Biosystems mass spectrometer. Optical rotation (α) of the racemic mixture was evaluated by a JASCO P-2000 optical activity polarimeter. Elemental analyses were carried out on a Carlo Erba model 1106; analyses indicated by the symbols of the elements were within ±0.4% of the theoretical values (see the Supporting Information). All reactions were followed by thin-

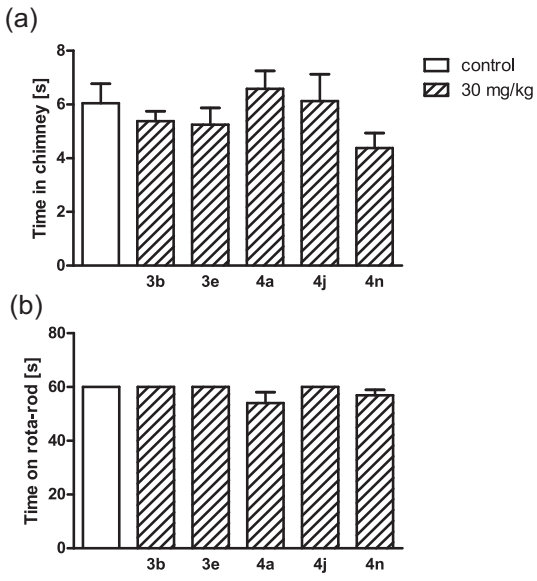

FIGURE 6 The influence of the tested compounds **3b**, **3e**, **4a**, **4j**, and **4n** (30 mg/kg) on motor coordination in mice evaluated in (a) chimney and (b) rotarod tests. Investigated compounds were injected intraperitoneally 60 min before the test. Data are expressed as mean ± *SEM* values of the one independent experiment (n = 7–9 mice). One-way analysis of variance did not show significant changes in the chimney ($F_{5,38}$ = 1.522; p = .2059) and the time spent on the rotarod ($F_{5,40}$ = 1.704; p = .1559)

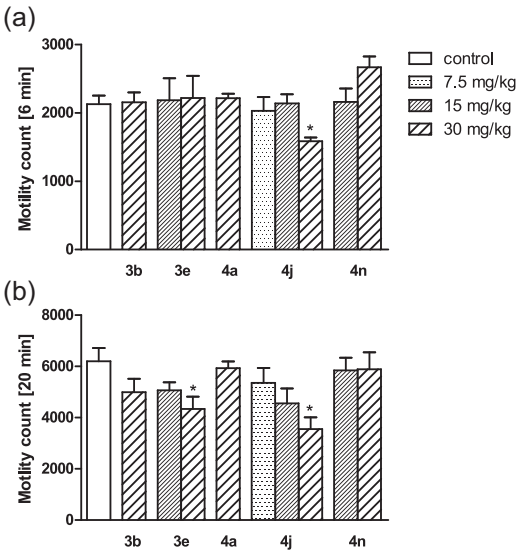

FIGURE 7 The influence of the tested compounds **3b**, **3e**, **4a**, **4j**, and **4n** (7.5–30 mg/kg) on the spontaneous locomotor activity of mice. Investigated compounds were injected intraperitoneally 60 min before the test. Locomotor activity was measured after 6 and 20 min. Data are expressed as mean ± *SEM* values of the one independent experiment (n = 7–9 mice); $^{*}p < .05$ versus control (Dunnett's test). One-way analysis of variance (ANOVA) showed significant changes in locomotor activity of mice in 6 min after administration of the compound **4j** ($F_{3,31} = 2.981$; $p < .05$). Dunnett's post hoc test confirmed a significant decrease in locomotor activity of mice after the administration of compound **4j** at the dose of 30 mg/kg ($p < .05$) after 6 min of observation. One-way ANOVA also revealed significant changes in locomotor activity of mice in 20 min after administration of the compound **3e** ($F_{2,17} = 4.234$; $p < .05$) and **4j** ($F_{3,23} = 3.795$; $p < .05$). Dunnett's post hoc test confirmed a significant decrease in locomotor activity of mice after the administration of compound **3e** at the doses of 30 ($p < .05$) and **4j** at the dose of 30 mg/kg ($p < .05$) after 20 min of observation

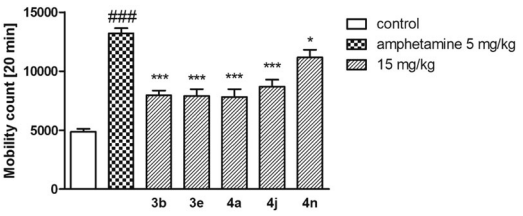

FIGURE 8 The influence of the tested compounds **3b**, **3e**, **4a**, **4j**, and **4n** (15 mg/kg) on the amphetamine-induced hyperactivity of mice. Compounds tested were injected 60 min and amphetamine 5 mg/kg 30 min before the test. Locomotor activity was measured for a period of 20 min. Data are expressed as mean ± *SEM* values of the one independent experiment (n = 7–9 mice); $^{###}p < .001$ versus control; $^{*}p < .05$ vs control (Dunnett's test); $^{***}p < .001$ versus amphetamine. One-way analysis of variance showed significant changes in the locomotor activity of mice ($F_{6,47} = 20.91$; $p < .001$). Dunnett's post hoc test confirmed a significant increase in locomotor activity of mice after the administration of amphetamine (5 mg/kg; $p < .001$). Moreover, all tested compounds at the dose of 15 mg/kg decreased amphetamine-induced hyperactivity of mice ($p < .001$ for compounds **3b**, **3e**, **4a**, **4j**, and $p < .05$ for compound **4n**)

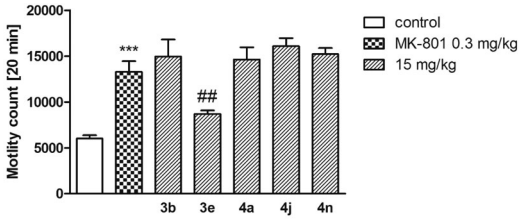

FIGURE 9 The influence of the tested compounds **3b**, **3e**, **4a**, **4j**, and **4n** (15 mg/kg) on the hyperactivity of mice provoked by an acute MK-801 (0.3 mg/kg, ip). The tested compounds were injected 60 min and MK-801 immediately before the test. Locomotor activity was measured for a period of 20 min. Data are expressed as mean ± *SEM* values of the one independent experiment (n = 7–9 mice); $^{***}p < .001$ versus control; $^{##}p < .001$ versus MK-801. One-way analysis of variance showed significant changes in the locomotor activity of mice ($F_{6,53} = 11.58$; $p < .001$). Dunnett's post hoc test confirmed a significant increase in locomotor activity of mice after the administration of MK-801 (0.3 mg/kg; $p < .001$). Moreover, compound**3e** at the dose of 15 mg/kg decreased MK-801-induced hyperactivity of mice ($p < .01$)

layer chromatography, carried out on Merck silica gel 60 F_{254} plates with a fluorescent indicator, and the plates were visualized with UV light (254 nm). Preparative chromatographic purifications were performed using a silica gel column (Kieselgel 60). Solutions were dried over Na_2SO_4 and concentrated with a Buchi R-114 rotary evaporator at low pressure.

The InChI codes of the investigated compounds, together with some biological activity data, are given as Supporting Information.

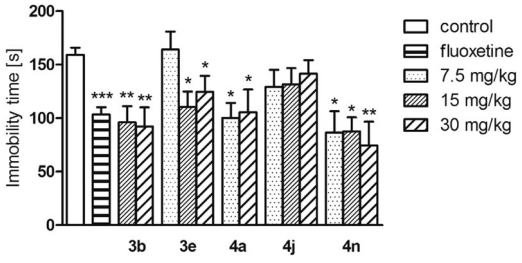

FIGURE 10 The influence of the investigated compounds **3b**, **3e**, **4a**, **4j**, and **4n** (7.5–30 mg/kg) and fluoxetine (15 mg/kg) on the total duration in the forced swim test (FST) in mice. The investigated compounds were administered intraperitoneally 60 min before the test. The values represent mean ± *SEM* of the one independent experiment (n = 7–9 mice); $^{*}p < .05$; $^{**}p < .01$ versus control (Dunnett's test). One-way analysis of variance showed significant changes in immobility time after administration of the compound **3b** ($F_{2,21} = 7.191$; $p < .01$), **3e** ($F_{3,23} = 3.775$; $p < .05$), **4a** ($F_{21} = 4.646$; $p < .05$), and **4j** ($F_{3,28} = 5.424$; $p < .01$). Dunnett's post hoc test confirmed a significant reduction in immobility time after the administration of compounds **3b** applied at doses of 15 and 30 mg/kg ($p < .01$), **3e** at doses of 15 and 30 mg/kg ($p < .05$), **4a** at doses of 15 and 30 mg/kg ($p < .05$), and **4n** applied at doses of 7.5 ($p < .05$), 15 ($p < .05$), and 30 mg/kg ($p < .01$). Also, fluoxetine (15 mg/kg) induced a significant reduction in the immobility time ($p < .001$)

4.1.2 | General procedure for the synthesis of 1-chloro-3-(4-substituted-arylpiperazin-1-yl)propan-2-ol (**2f–n**)

To a solution of the appropriate 4-substituted arylpiperazine (**1**) (1 g; 0.005 mol) in absolute ethanol (35 ml), epichlorohydrin (0.462 g; 0.005 mol) was added dropwise, and the reaction mixture was stirred overnight at room temperature. After evaporation, the crude products were recrystallized from diethyl ether to give intermediates **2f–n** as solids (yield ranging between 55% and 71%). ^{1}H NMR spectra for all intermediates were consistent with the proposed structures.

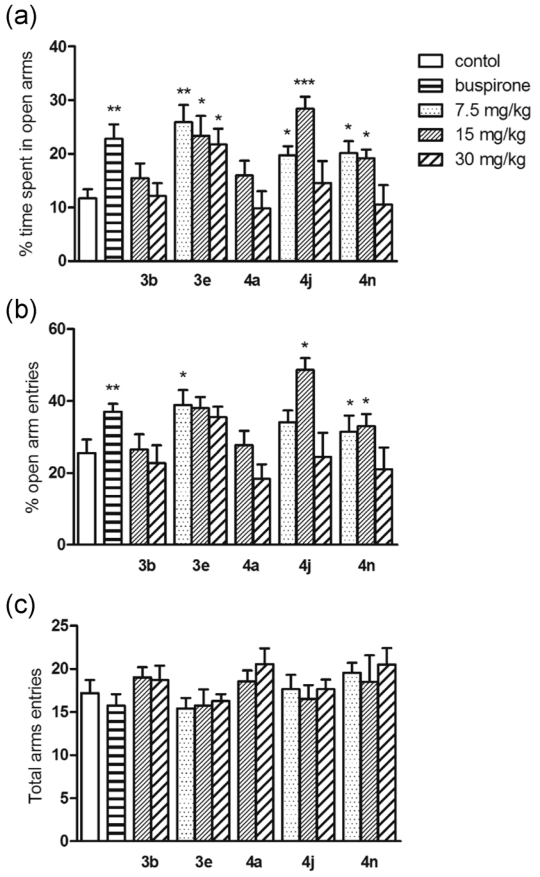

FIGURE 11 The influence of the investigated compounds **3b**, **3e**, **4a**, **4j**, and **4n** (7.5–30 mg/kg) on elevated plus-maze (EPM) performance in mice. (a) Percentage of time spent in open arms, (b) the percentage of the open arm entries, and (c) total arm entries. Investigated compounds were injected intraperitoneally 60 min before the test. The results are expressed as mean ± *SEM* of the one independent experiment (n = 7–9 mice); ***p < .001; **p < .01; *p < .05 versus control (Dunnett's test). One-way analysis of variance showed significant changes in (a) the percentage of time spent in open arms of EPM (**3e** $F_{3,30}$ = 5.471; p < .01; **4j** $F_{3,30}$ = 7.961; p < .001; **4n** $F_{3,31}$ = 4.34; p < .05) and in (b) the percentage of open arm entries (**3e** $F_{3,30}$ = 3.009; p < .05; **4j** $F_{3,30}$ = 4.219; p < .05; **4n** $F_{3,31}$ = 3.215; p < .05). There were no significant changes in (c) the total arm entries ($F_{14,89}$ = 1.097; p = .3719). Dunnett's post hoc test confirmed a significant increase in time spent in open arms after the administration of compounds: **3e** at doses of 7.5 (p < .01), 15 (p < .05), and 30 mg/kg (p < .05); **4j** at doses of 7.5 (p < .05) and 15 mg/kg (p < .001), and **4n** at doses of 7.5 and 15 mg/kg (p < .05). These compounds were also able to increase the percentage of open arm entries: **3e** at the dose of 7.5 mg/kg (p < .05), **4j** at the dose of 15 mg/kg (p < .05), and **4n** at doses of 7.5 and 15 mg/kg (p < .05). Also, buspirone (5 mg/kg) induced a significant increase in the percentage of time spent in open arms and in the percentage of open arms entries (p < .01)

4.1.3 | General procedure for the reaction of *endo*-*N*-hydroxy-5-norbornene-2,3-dicarboximide and *exo*-*N*-hydroxy-7-oxabicyclo[2.2.1]hept-5-ene-2,3-dicarboximide with derivatives **2f–n** (**3f–n**; **4f–n**)

A solution of absolute ethanol (35 ml) and 0.2 g (0.05 mol) of sodium hydroxide was reacted with 1 g (0.005 mol) of commercially available *endo*-*N*-hydroxy-5-norbornene-2,3-dicarboximide or *exo*-*N*-hydroxy-7-oxabicyclo[2.2.1]hept-5-ene-2,3-dicarboximide and 1.420 g (0.005 mol) of the appropriate 1-chloro-3-(4-substituted-arylpiperazin-1-yl)propan-2-ol (**2f–n**) at 70°C for 24 h. Afterward, the mixture was cooled to room temperature, concentrated to dryness, and the residue was diluted in water (40 ml). The solution was extracted several times with CH_2Cl_2. The combined organic layers were dried on anhydrous Na_2SO_4 and concentrated in vacuo. The residue was purified by column chromatography (CH_2Cl_2/methanol 9:1 v/v). The combined and evaporated product fractions were crystallized from diethyl ether, yielding the desired products (**3f–n** and **4f–n**) as white solids.

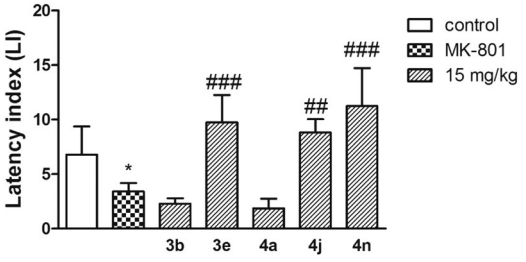

FIGURE 12 The influence of the investigated compounds **3b**, **3e**, **4a**, **4j**, and **4n** (15 mg/kg) on the memory impairment provoked by an acute administration of MK-801 (0.3 mg/kg, ip) in the passive avoidance test in mice. The investigated compounds were administered intraperitoneally, immediately after the training. The values represent mean ± *SEM* of the one independent experiment (n = 13 mice); *p < .05 versus control; ##p < .01, ###p < .001 versus MK-801 (Dunnett's test). One-way analysis of variance revealed a statistically significant effect on the latency index (LI) values for consolidation of long-term memory ($F_{6,84}$ = 3.511; p < .01). Post hoc Dunnett's test indicated that treatment with MK-801 (0.3 mg/kg, ip) significantly decreased LI values in mice as compared with the control group (p < .05). These data showed that MK-801, at the dose of 0.3 mg/kg, impaired consolidation of long-term memory. Moreover, an acute injection of **3e** (p < .001), **4j** (p < .01), and **4n** (p < .001) attenuated the amnestic effect of MK-801

4.1.4 | Synthesis of 4-{3-[4-(*p*-methoxyphenyl)-piperazin-1-yl]propoxy-2-ol}-4-aza-tricyclo[5.2.1.02,6]-dec-8-ene-3,5-dione (**3f**)

From **2f** and *endo*-*N*-hydroxy-5-norbornene-2,3-dicarboximide. Yield: 77%; mp: 124–125°C. ^{1}H NMR (400 MHz, $CDCl_3$) δ: 1.50 (d, 1H, J = 8.9); 1.76 (d, 1H, J = 8.9); 2.47 (dd, 1H, CH_2–N, J = 4.0, J = 8.8); 2.55 (dd, 1H, CH_2–N, J = 4.2, J = 8.1); 2.65 (bs, 2H, CH_2 pip); 2.73 (bs, 2H, CH_2 pip); 3.07 (bs, 4H, $2CH_2$ pip); 3.21 (s, 2H); 3.43 (s, 2H); 3.76 (s, 3H, $-OCH_3$); 3.89–3.93 (m, 1H, CH–OH); 4.06 (dd, 2H, O–CH_2, J = 3.0, J = 7.0); 6.16 (s, 2H); 6.82 (d, 2H); 6.87 (d, 2H). Electrospray ionization–mass spectrometry (ESI-MS): 428.1 $[M+H]^+$; 450.4 $[M+Na]^+$; 466.4 $[M+K]^+$ (calcd: 427.49). Anal. ($C_{23}H_{29}N_3O_5$), C, H, N.

4.1.5 | Synthesis of 4-{3-[4-(*o*-chlorophenyl)-piperazin-1-yl]propoxy-2-ol}-4-aza-tricyclo[5.2.1.02,6]-dec-8-ene-3,5-dione (**3g**)

From **2g** and *endo*-*N*-hydroxy-5-norbornene-2,3-dicarboximide. Yield: 83%; mp: 125–127°C. ^{1}H NMR (400 MHz, $CDCl_3$) δ: 1.50 (d, 1H, J = 8.9); 1.76 (d, 1H, J = 8.9); 2.46 (dd, 1H, CH_2–N, J = 4.0, J = 8.8); 2.56 (dd, 1H, CH_2–N, J = 4.2, J = 8.1); 2.67 (bs, 2H, CH_2 pip); 2.75 (bs, 2H, CH_2 pip); 3.06 (bs, 4H, $2CH_2$ pip); 3.22 (s, 2H); 3.44 (s, 2H); 3.89–3.94 (m, 1H, CH–OH); 4.08 (dd, 2H, O–CH_2, J = 3.0, J = 7.0); 6.17 (s, 2H); 6.97 (t, 1H); 7.02 (d, 1H); 7.21 (t, 1H); 7.34 (d, 1H). ESI-MS: 432.3 $[M+H]^+$; 454.1 $[M+Na]^+$; 470.1 $[M+K]^+$ (calcd: 431.91). Anal. ($C_{22}H_{26}ClN_3O_4$), C, H, N.

4.1.6 | Synthesis of 4-{3-[4-(*m*-chlorophenyl)-piperazin-1-yl]propoxy-2-ol}-4-aza-tricyclo[5.2.1.02,6]-dec-8-ene-3,5-dione (**3h**)

From **2h** and *endo*-*N*-hydroxy-5-norbornene-2,3-dicarboximide. Yield: 70%; mp: 100–102°C. ^{1}H NMR (400 MHz, $CDCl_3$) δ: 1.51 (d, 1H, J = 8.9); 1.77 (d, 1H, J = 8.9); 2.46 (dd, 1H, CH_2–N, J = 4.0, J = 8.8); 2.55 (dd, 1H, CH_2–N, J = 4.2, J = 8.1); 2.63 (bs, 2H, CH_2 pip); 2.70 (bs, 2H, CH_2 pip); 3.18 (bs, 4H, $2CH_2$ pip); 3.21 (s, 2H); 3.44 (s, 2H); 3.89–3.93 (m, 1H, CH–OH); 4.07 (dd, 2H, O–CH_2, J = 3.0, J = 7.0); 6.17 (s, 2H); 6.76–6.81 (m, 2H, J = 7.6); 6.85 (s, 1H); 7.15 (t, 1H). ESI-MS: 432.1 $[M+H]^+$; 454.1 $[M+Na]^+$; 470.1 $[M+K]^+$ (calcd: 431.91). Anal. ($C_{22}H_{26}ClN_3O_4$), C, H, N.

4.1.7 | Synthesis of 4-{3-[4-(3,4-dichlorophenyl)-piperazin-1-yl]propoxy-2-ol}-4-aza-tricyclo[5.2.1.02,6]-dec-8-ene-3,5-dione (**3i**)

From **2i** and *endo*-*N*-hydroxy-5-norbornene-2,3-dicarboximide. Yield: 74%; mp: 160–162°C. ^{1}H NMR (400 MHz, $CDCl_3$) δ: 1.51 (d, 1H, J = 8.9); 1.77 (d, 1H, J = 8.9); 2.46 (dd, 1H, CH_2–N, J = 4.0, J = 8.8); 2.55 (dd, 1H, CH_2–N, J = 4.2, J = 8.1); 2.63 (bs, 2H, CH_2 pip); 2.69 (bs, 2H, CH_2 pip); 3.15 (bs, 4H, $2CH_2$ pip); 3.22 (s, 2H); 3.44 (s, 2H); 3.89–3.93 (m, 1H, CH–OH); 4.07 (dd, 2H, O–CH_2, J = 3.0, J = 7.0); 6.16 (s, 2H); 6.70 (dd, 1H); 6.93 (d, 1H); 7.25 (d, 1H, J = 7.3). ESI-MS: 467.0 $[M+H]^+$; 489.8 $[M+Na]^+$; 505.8 $[M+K]^+$ (calcd: 466.36). Anal. ($C_{22}H_{25}Cl_2N_3O_4$), C, H, N.

4.1.8 | Synthesis of 4-{3-[4-(pyridin-2-yl)piperazin-1-yl]propoxy-2-ol}-4-aza-tricyclo[5.2.1.02,6]dec-8-ene-3,5-dione (**3j**)

From **2j** and *endo*-*N*-hydroxy-5-norbornene-2,3-dicarboximide. Yield: 61%; mp: 145–146°C; ^{1}H NMR (400 MHz, $CDCl_3$) δ: 1.50 (d, 1H, J = 8.9); 1.76 (d, 1H, J = 8.9); 2.44 (dd, 1H, CH_2–N, J = 4.0, J = 8.8); 2.54 (dd, 1H, CH_2–N, J = 4.2, J = 8.1); 2.59 (bs, 2H, CH_2 pip); 2.66 (bs, 2H, CH_2 pip); 3.21 (s, 2H); 3.43 (s, 2H); 3.52 (bs, 4H, $2CH_2$ pip); 3.89–3.93 (m, 1H, CH–OH); 4.08 (dd, 2H, O–CH_2, J = 3.0, J = 7.0); 6.16 (s, 2H); 6.60–6.64 (m, 2H); 7.44–7.49 (m, 1H); 8.17 (dd, 1H). ESI-MS: 399.2 $[M+H]^+$; 421.3 $[M+Na]^+$; 437.4 $[M+K]^+$ (calcd: 398.46). Anal. ($C_{21}H_{26}N_4O_4$), C, H, N.

4.1.9 | Synthesis of 4-{3-[4-(pyrimidin-2-yl)-piperazin-1-yl]propoxy-2-ol}-4-aza-tricyclo[5.2.1.02,6]-dec-8-ene-3,5-dione (**3k**)

From **2k** and *endo*-*N*-hydroxy-5-norbornene-2,3-dicarboximide. Yield: 65%; mp: 177–179°C; ^{1}H NMR (400 MHz, $CDCl_3$) δ: 1.50 (d, 1H, J = 8.9); 1.76 (d, 1H, J = 8.9); 2.43 (dd, 1H, CH_2–N, J = 4.0, J = 8.8); 2.50 (dd, 1H, CH_2–N, J = 4.2, J = 8.1); 2.54 (bs, 2H, CH_2 pip); 2.61 (bs, 2H, CH_2 pip); 3.21 (s, 2H); 3.44 (s, 2H); 3.81 (bs, 4H, $2CH_2$ pip); 3.89–3.93 (m, 1H, CH–OH); 4.07 (dd, 2H, O–CH_2, J = 3.0, J = 7.0); 6.16 (s, 2H); 6.48 (t, 1H); 8.29 (d, 2H). ESI-MS: 400.3 $[M+H]^+$; 422.1 $[M+Na]^+$; 438.0 $[M+K]^+$ (calcd: 399.44). Anal. ($C_{20}H_{25}N_5O_4$), C, H, N.

4.1.10 | Synthesis of 4-{3-[4-(piperonyl)piperazin-1-yl]propoxy-2-ol}-4-aza-tricyclo[5.2.1.02,6]dec-8-ene-3,5-dione (**3l**)

From **2l** and *endo*-*N*-hydroxy-5-norbornene-2,3-dicarboximide. Yield: 40%; mp: 110–111°C; ^{1}H NMR (400 MHz, $CDCl_3$) δ: 1.50 (d, 1H, J = 8.9); 1.75 (d, 1H, J = 8.9); 2.37–2.58 (m, 10H); 3.19 (s, 2H); 3.39 (s, 2H, $-CH_2$); 3.42 (s, 2H); 3.85–3.89 (m, 1H, CH–OH); 4.03 (dd, 2H, O–CH_2, J = 3.0, J = 7.0); 5.93 (s, 2H); 6.14 (s, 2H); 6.73 (s, 2H); 6.83 (s, 1H). ESI-MS: 455.9 $[M+H]^+$; 478.2 $[M+Na]^+$; 494.3 $[M+K]^+$ (calcd: 455.5). Anal. ($C_{24}H_{29}N_3O_6$), C, H, N.

4.1.11 | Synthesis of 4-{3-[4-(thiophen-2-ylmethyl)-piperazin-1-yl]propoxy-2-ol}-4-aza-tricyclo[5.2.1.02,6]-dec-8-ene-3,5-dione (**3m**)

From **2m** and *endo*-*N*-hydroxy-5-norbornene-2,3-dicarboximide. Yield: 55%; mp: 118–120°C; ^{1}H NMR (400 MHz, $CDCl_3$) δ: 1.49 (d,

1H, *J* = 8.9); 1.75 (d, 1H, *J* = 8.9); 2.38–2.60 (m, 10H); 3.19 (s, 2H); 3.42 (s, 2H); 3.71 (s, 2H, $-CH_2$); 3.85–3.88 (m, 1H, CH–OH); 4.03 (dd, 2H, O–CH_2, *J* = 3.0, *J* = 7.0); 6.14 (s, 2H); 6.90–6.94 (m, 2H); 7.22 (d, 1H). ESI-MS: 418.3 $[M+H]^+$; 440.2 $[M+Na]^+$; 456.2 $[M+K]^+$ (calcd: 417.52). Anal. ($C_{21}H_{27}N_3O_4S$), C, H, N.

4.1.12 | Synthesis of 4-{3-[4-(naphthalen-1-yl)-piperazin-1-yl]propoxy-2-ol}-4-aza-tricyclo[5.2.1.02,6]-dec-8-ene-3,5-dione (**3n**)

From **2n** and *endo*-*N*-hydroxy-5-norbornene-2,3-dicarboximide. Yield: 77%; mp: 87–89°C. ^{1}H NMR (400 MHz, $CDCl_3$) *δ*: 1.50 (d, 1H, *J* = 8.9); 1.77 (d, 1H, *J* = 8.9); 2.56 (dd, 1H, CH_2–N, *J* = 4.0, *J* = 8.8); 2.63 (dd, 1H, CH_2–N, *J* = 4.2, *J* = 8.1); 2.78 (bs, 2H, CH_2 pip); 2.87 (bs, 2H, CH_2 pip); 3.13 (bs, 4H, $2CH_2$ pip); 3.22 (s, 2H); 3.44 (s, 2H); 3.93–3.97 (m, 1H, CH–OH); 4.10 (dd, 2H, O–CH_2, *J* = 3.0, *J* = 7.0); 6.18 (s, 2H); 7.07 (d, 1H); 7.39 (t, 1H); 7.46 (m, 2H); 7.54 (d, 1H); 7.81 (d, 1H); 8.17 (d, 1H). ESI-MS: 448.1 $[M+H]^+$; 470.2 $[M+Na]^+$; 486.2 $[M+K]^+$ (calcd: 447.53). Anal. ($C_{26}H_{29}N_3O_4$), C, H, N.

4.1.13 | Synthesis of 4-{3-[4-(*p*-methoxyphenyl)-piperazin-1-yl]propoxy-2-ol}-10-oxa-4-aza-tricyclo-[5.2.1.02,6]dec-8-ene-3,5-dione (**4f**)

From **2f** and *exo*-*N*-hydroxy-7-oxabicyclo[2.2.1]hept-5-ene-2,3-dicarboximide. Yield: 53%; mp: 141–143°C. ^{1}H NMR (400 MHz, $CDCl_3$) *δ*: 2.49 (dd, 1H, CH_2–N, *J* = 4.0, *J* = 8.8); 2.61 (dd, 1H, CH_2–N, *J* = 4.2, *J* = 8.1); 2.64 (bs, 2H, CH_2 pip); 2.73 (bs, 2H, CH_2 pip); 2.78 (s, 2H); 3.07 (bs, 4H, $2CH_2$ pip); 3.76 (s, 3H, $-OCH_3$); 4.01–4.03 (m, 1H, CH–OH); 4.20 (d, 2H, O–CH_2, *J* = 8.1); 5.28 (d, 2H, *J* = 4.8); 6.51 (s, 2H); 6.81 (d, 2H); 6.87 (d, 2H). ESI-MS: 430.2 $[M+H]^+$; 452.2 $[M+Na]^+$; 468.2 $[M+K]^+$ (calcd: 429.47). Anal. ($C_{22}H_{27}N_3O_6$), C, H, N.

4.1.14 | Synthesis of 4-{3-[4-(*o*-chlorophenyl)-piperazin-1-yl]propoxy-2-ol}-10-oxa-4-aza-tricyclo-[5.2.1.02,6]dec-8-ene-3,5-dione (**4g**)

From **2g** and *exo*-*N*-hydroxy-7-oxabicyclo[2.2.1]hept-5-ene-2,3-dicarboximide. Yield: 30%; mp: 121–122°C. ^{1}H NMR (400 MHz, $CDCl_3$) *δ*: 2.48 (dd, 1H, CH_2–N, *J* = 4.0, *J* = 8.8); 2.57 (dd, 1H, CH_2–N, *J* = 4.2, *J* = 8.1); 2.63–2.67 (m, 4H, CH_2 pip); 2.79 (bs, 4H, $2CH_2$ pip); 3.06 (s, 2H); 4.02–4.06 (m, 1H, CH–OH); 4.21 (d, 2H, O–CH_2, *J* = 8.1); 5.29 (d, 2H, *J* = 4.8); 6.52 (s, 2H); 6.96 (t, 1H); 7.02 (d, 1H); 7.21 (t, 1H); 7.34 (d, 1H). ESI-MS: 434.3 $[M+H]^+$; 456.2 $[M+Na]^+$; 472.2 $[M+K]^+$ (calcd: 433.89). Anal. ($C_{21}H_{24}ClN_3O_5$), C, H, N.

4.1.15 | Synthesis of 4-{3-[4-(*m*-chlorophenyl) piperazin-1-yl]propoxy-2-ol}-10-oxa-4-aza-tricyclo-[5.2.1.02,6]dec-8-ene-3,5-dione (**4h**)

From **2h** and *exo*-*N*-hydroxy-7-oxabicyclo[2.2.1]hept-5-ene-2,3-dicarboximide. Yield: 42%; mp: 113–115°C. ^{1}H NMR (400 MHz, $CDCl_3$) *δ*: 2.46 (dd, 1H, CH_2–N, *J* = 4.0, *J* = 8.8); 2.56 (dd, 1H, CH_2–N, *J* = 4.2, *J* = 8.1); 2.63 (bs, 2H, CH_2 pip); 2.70 (bs, 2H, CH_2 pip); 2.79 (s, 2H); 3.17 (bs, 4H, $2CH_2$ pip); 4.01–4.05 (m, 1H, CH–OH); 4.21 (d, 2H, O–CH_2, *J* = 8.1); 5.29 (d, 2H, *J* = 4.8); 6.52 (s, 2H); 6.76–6.81 (m, 2H, *J* = 7.3); 6.85 (s, 1H); 7.15 (t, 1H). ESI-MS: 434.3 $[M+H]^+$; 456.2 $[M+Na]^+$; 472.2 $[M+K]^+$ (calcd: 433.89). Anal. ($C_{21}H_{24}ClN_3O_5$), C, H, N.

4.1.16 | Synthesis of 4-{3-[4-(3,4-dichlorophenyl)-piperazin-1-yl]propoxy-2-ol}-10-oxa-4-aza-tricyclo-[5.2.1.02,6]dec-8-ene-3,5-dione (**4i**)

From **2i** and *exo*-*N*-hydroxy-7-oxabicyclo[2.2.1]hept-5-ene-2,3-dicarboximide. Yield: 24%; mp: 141–143°C. ^{1}H NMR (400 MHz, $CDCl_3$) *δ*: 2.46 (dd, 1H, CH_2–N, *J* = 4.0, *J* = 8.8); 2.56 (dd, 1H, CH_2–N, *J* = 4.2, *J* = 8.1); 2.62 (bs, 2H, CH_2 pip); 2.69 (bs, 2H, CH_2 pip); 2.79 (s, 2H); 3.15 (bs, 4H, $2CH_2$ pip); 4.00–4.05 (m, 1H, CH–OH); 4.21 (d, 2H, O–CH_2, *J* = 8.1); 5.29 (d, 2H, *J* = 4.8); 6.52 (s, 2H); 6.70 (dd, 1H, *J* = 7.3); 6.93 (d, 1H, *J* = 7.3); 7.25 (d, 1H). ESI-MS: 469.3 $[M+H]^+$ (calcd: 468.33). Anal. ($C_{21}H_{23}Cl_2N_3O_5$), C, H, N.

4.1.17 | Synthesis of 4-{3-[4-(pyridin-2-yl)piperazin-1-yl]propoxy-2-ol}-10-oxa-4-aza-tricyclo[5.2.1.02,6]-dec-8-ene-3,5-dione (**4j**)

From **2j** and *exo*-*N*-hydroxy-7-oxabicyclo[2.2.1]hept-5-ene-2,3-dicarboximide. Yield: 27%; mp: 145–146°C. ^{1}H NMR (400 MHz, $CDCl_3$) 2.45 (dd, 1H, CH_2–N, *J* = 4.0, *J* = 8.8); 2.55 (dd, 1H, CH_2–N, *J* = 4.2, *J* = 8.1); 2.60 (bs, 2H, CH_2 pip); 2.67 (bs, 2H, CH_2 pip); 2.79 (s, 2H); 3.52 (bs, 4H, $2CH_2$ pip); 4.00–4.05 (m, 1H, CH–OH); 4.21 (d, 2H, O–CH_2, *J* = 8.2); 5.29 (d, 2H, *J* = 4.4); 6.52 (s, 2H); 6.60–6.64 (m, 2H); 7.44–7.49 (m, 1H); 8.17 (dd, 1H). ESI-MS: 401.3 $[M+H]^+$; 423.3 $[M+Na]^+$; 439.0 $[M+K]^+$ (calcd: 400.43). Anal. ($C_{20}H_{24}N_4O_5$), C, H, N.

4.1.18 | Synthesis of 4-{3-[4-(pyrimidin-2-yl)-piperazin-1-yl]propoxy-2-ol}-10-oxa-4-aza-tricyclo-[5.2.1.02,6]dec-8-ene-3,5-dione (**4k**)

From **2k** and *exo*-*N*-hydroxy-7-oxabicyclo[2.2.1]hept-5-ene-2,3-dicarboximide. Yield: 58%; mp: 149–151°C; ^{1}H NMR (400 MHz, $CDCl_3$) *δ*: 2.43 (dd, 1H, CH_2–N, *J* = 4.0, *J* = 8.8); 2.49 (dd, 1H, CH_2–N, *J* = 4.2, *J* = 8.1); 2.53 (bs, 2H, CH_2 pip); 2.61 (bs, 2H, CH_2 pip); 2.79 (s,

2H); 3.81 (bs, 4H, $2CH_2$ pip); 4.02–4.05 (m, 1H, CH–OH); 4.22 (d, 2H, O–CH_2, J = 3.0, J = 7.0); 5.29 (d, 2H); 6.48 (t, 1H); 6.52 (s, 2H); 8.29 (d, 2H). ESI-MS: 402.4 $[M+H]^+$; 424.2 $[M+Na]^+$; 440.1 $[M+K]^+$ (calcd: 401.42). Anal. ($C_{19}H_{23}N_5O_5$), C, H, N.

4.1.19 | Synthesis of 4-{3-[4-(piperonyl)piperazin-1-yl]propoxy-2-ol}-10-oxa-4-aza-tricyclo[5.2.1.02,6]dec-8-ene-3,5-dione (**4l**)

From **2l** and *exo*-*N*-hydroxy-7-oxabicyclo[2.2.1]hept-5-ene-2,3-dicarboximide. Yield: 70%; mp: 144–146°C; ^{1}H NMR (400 MHz, $CDCl_3$) δ: 2.37–2.59 (m, 10H); 2.77 (s, 2H); 3.39 (s, 2H, $-CH_2$); 3.96–4.02 (m, 1H, CH–OH); 4.15 (dd, 2H, O–CH_2, J = 3.0, J = 7.0); 5.28 (d, 2H); 5.93 (s, 2H); 6.51 (s, 2H); 6.73 (s, 2H); 6.83 (s, 1H). ESI-MS: 458.1 $[M+H]^+$; 480.2 $[M+Na]^+$; 496.2 $[M+K]^+$ (calcd: 457.48). Anal. ($C_{23}H_{27}N_3O_7$), C, H, N.

4.1.20 | Synthesis of 4-{3-[4-(thiophen-2-ylmethyl)-piperazin-1-yl]propoxy-2-ol}-10-oxa-4-aza-tricyclo-[5.2.1.02,6]dec-8-ene-3,5-dione (**4m**)

From **2m** and *exo*-*N*-hydroxy-7-oxabicyclo[2.2.1]hept-5-ene-2,3-dicarboximide. Yield: 60%; mp: 122–124°C; ^{1}H NMR (400 MHz, $CDCl_3$) δ: 2.39–2.62 (m, 10H); 2.78 (s, 2H); 3.71 (s, 2H, $-CH_2$); 3.95–4.02 (m, 1H, CH–OH); 4.15 (d, 2H, O–CH_2, J = 3.0, J = 7.0); 5.28 (d, 2H); 6.51 (s, 2H); 6.90–6.95 (m, 2H); 7.22 (d, 1H). ESI-MS: 420.2 $[M+H]^+$; 442.3 $[M+Na]^+$; 458.3 $[M+K]^+$ (calcd: 419.49). Anal. ($C_{20}H_{25}N_3O_5S$), C, H, N.

4.1.21 | Synthesis of 4-{3-[4-(naphthalen-1-yl)-piperazin-1-yl]propoxy-2-ol}-10-oxa-4-aza-tricyclo-[5.2.1.02,6]dec-8-ene-3,5-dione (**4n**)

From **2n** and *exo*-*N*-hydroxy-7-oxabicyclo[2.2.1]hept-5-ene-2,3-dicarboximide. Yield: 53%; mp: 70–71°C. ^{1}H NMR (400 MHz, $CDCl_3$) δ: 2.57 (dd, 1H, CH_2–N, J = 4.0, J = 8.8); 2.64 (dd, 1H, CH_2–N, J = 4.2, J = 8.1); 2.79 (bs, 4H); 2.87 (bs, 2H, CH_2 pip); 3.13 (bs, 4H, $2CH_2$ pip); 4.06–4.09 (m, 1H, CH–OH); 4.25 (d, 2H, O–CH_2, J = 8.1); 5.30 (d, 2H, J = 4.8); 6.52 (s, 2H); 7.07 (d, 1H); 7.39 (t, 1H); 7.46 (m, 2H); 7.54 (d, 1H); 7.81 (d, 1H); 8.17 (d, 1H). ESI-MS: 450.5 $[M+H]^+$; 474.6 $[M+Na]^+$; 488.4 $[M+K]^+$ (calcd: 449.5). Anal. ($C_{25}H_{27}N_3O_5$), C, H, N.

4.2 | In vitro receptor assays

4.2.1 | Functional 5-HT_{1A} receptor assay

Male Sprague–Dawley (SD) rats were decapitated and their brains removed and placed on ice. Hippocampi were dissected and homogenized with a glass homogenizer in 30 vol ice-cold TED buffer (50 mM Tris-HCl, 1 mM EDTA, 1 mM dithiothreitol, pH 7.4). Next, the homogenate was centrifuged at 21,000*g* for 30 min at 4°C. The pellet was suspended in 30 vol TED buffer (pH 7.4) and incubated in a water bath for 10 min at 37°C to remove endogenous ligands. The suspension was centrifuged again at 21,000*g* for 30 min at 4°C. The pellet was resuspended in 30 vol TED buffer (pH 7.4) and the centrifugation step was repeated. The final pellet was suspended in 10 vol 50 mM Tris-HCl (pH 7.4) and stored at −80°C until use. In the agonist mode, 15 μg/ml of hippocampus homogenate was incubated in triplicate with 0.8 nM [^{35}S]GTPγS in an assay buffer (50 mM Tris-HCl, pH 7.4, 1 mM EGTA, 3 mM $MgCl_2$, 100 mM NaCl, 30 μM GDP) in the presence of increasing concentrations of the tested compounds (10^{-10} to 10^{-5} M). In the antagonist mode, compounds were additionally incubated with 100 nM 8-OH-DPAT. Nonspecific binding was determined with 100 μM of unlabeled GTPγS. The reaction mixture was incubated for 90 min at 37°C in a volume of 250 μl. Next, 96-well Unifilter® Plates (PerkinElmer) were presoaked for 1 h with 50 mM Tris-HCl (pH 7.4) before harvesting. The reaction was terminated by vacuum filtration on filter plates with the FilterMate Harvester® (PerkinElmer). The samples were then rapidly washed with 2 ml of 50 mM Tris-HCl (pH 7.4) buffer. Filter plates were dried for 2 h at 50°C. After drying, 45 μl of EcoScint-20 scintillant (PerkinElmer) was added to every well. Radioactivity was counted in a Trilux MicroBeta^2 counter (PerkinElmer). Data were analyzed with GraphPad Prism 5.0 software (GraphPad Software; www.graphpad.com). Curves were fitted with a one-site nonlinear regression model. Efficacy (E_{max}) and potency (pEC_{50} for agonists; pIC_{50} and pK_B for antagonists) were calculated from the Cheng–Prusoff and Gaddum/Schild models and expressed as mean ± *SEM*. Differences in compound potency and efficacy were evaluated with the extra sum-of-squares *F* test. Baseline G-protein stimulation was set to 100%. One, two, or three symbols represent statistical significance of 0.05, 0.01, and 0.001, respectively. Differences in potency and efficacy between the ligands were analyzed with the extra sum-of-squares *F* test.

4.2.2 | 5-HT_{2A} competition binding assay

Male SD rats were decapitated and their brains removed and placed on ice. Frontal cortices were homogenized with a glass homogenizer in 30 vol ice-cold homogenization buffer (50 mM Tris-HCl, 1 mM EDTA, 5 mM $MgCl_2$, pH 7.4). Next, the homogenate was centrifuged at 20,000*g* for 15 min at 4°C. The pellet was suspended in 30 vol 50 mM Tris-HCl (pH 7.4) and incubated in a water bath for 15 min at 37°C to remove endogenous serotonin. The suspension was again centrifuged at 20,000*g* for 15 min at 4°C. The pellet was resuspended in 10 vol 50 mM Tris-HCl (pH 7.4) and the centrifugation step was repeated. The final pellet was suspended in 10 vol 50 mM Tris-HCl (pH 7.4) and stored at −80°C. For the 5-HT_{2A} assay, frontal cortex homogenates (160 μg protein/ml) were incubated in triplicate with 1 nM [^{3}H]ketanserin for 60 min at 36°C in a 50 mM Tris-HCl (pH 7.4) buffer containing 0.1% ascorbate, 3 mM $CaCl_2$, and 10 μM pargyline, and increasing concentrations (10^{-9} to 10^{-5} M) of the

compound of interest. Nonspecific binding was determined in the presence of 10 μM mianserin. After incubation, the reaction mixture was deposited on UniFilter-96 GF/B plates with the aid of a FilterMate-96 Harvester. Filter plates were presoaked beforehand with 0.4% polyethylenimine (PEI) for 1 h. Next, each filter well was washed with 1.75 ml of 50 mM Tris-HCl (pH 7.4) and left to dry on a heating block set to 50°C for 2 h. Then, 45 μl of Microscint-20 scintillation fluid was added to each filter well and left to equilibrate overnight. Filter-bound radioactivity was counted in a MicroBeta^2 Microplate Counter. Binding curves were fitted with a one-site nonlinear regression model. Inhibition curves were fitted with a one-site nonlinear regression model. Affinity was presented as the inhibitory constant (pK_i and $K_i \pm SEM$) from two or three separate experiments. Differences in K_i values were evaluated with the extra sum-of-squares *F* test. One, two, or three symbols represent statistical significance of 0.05, 0.01, and 0.001, respectively.

4.2.3 | 5-HT$_{2C}$ competition binding assay

Male SD rats were decapitated and their brains removed and placed on ice. Frontal cortices were homogenized with a glass homogenizer in 30 vol ice-cold homogenization buffer (50 mM Tris-HCl, 10 mM $MgCl_2$, pH 7.4). Next, the homogenate was centrifuged at 20,000*g* for 15 min at 4°C. The pellet was suspended in 30 vol 50 mM Tris-HCl (pH 7.4) and incubated in a water bath for 15 min at 37°C to remove endogenous serotonin. The suspension was again centrifuged at 20,000*g* for 15 min at 4°C. The pellet was resuspended in 10 vol 50 mM Tris-HCl (pH 7.4) and the centrifugation step was repeated. The final pellet was suspended in 10 vol 50 mM Tris-HCl (pH 7.4) and stored at −80°C. For the 5-HT$_{2C}$ assay, frontal cortex homogenates (250 μg protein/ml) were incubated in triplicate with 1 nM [^{3}H]mesulergine for 60 min at 36°C in a 50 mM Tris-HCl (pH 7.4) buffer containing 0.1% ascorbate, 10 mM $MgCl_2$, 10 μM pargyline, 100 nM spiperone, and increasing concentrations (10^{-9} to 10^{-5} M) of the compound tested. Nonspecific binding was determined in the presence of 10 μM mianserin. After incubation, the reaction mixture was deposited on UniFilter-96 GF/B plates with the aid of a FilterMate-96 Harvester. Filter plates were presoaked beforehand with 0.4% PEI for 1 h. Next, each filter well was washed with 1.75 ml of 50 mM Tris-HCl (pH 7.4) and left to dry for 2 h on a heating block set to 50°C. Then, 45 μl of Microscint-20 scintillation fluid was added to each filter well and left to equilibrate overnight. Filter-bound radioactivity was counted in a MicroBeta^2 Microplate Counter. Binding curves were fitted with a one-site nonlinear regression model. Affinity was presented as the inhibitory constant (pK_i and $K_i \pm SEM$) from two or three separate experiments. Differences in K_i values were evaluated with the extra sum-of-squares *F* test. One, two, or three symbols represent statistical significance of 0.05, 0.01, and 0.001, respectively.

4.2.4 | Functional D$_2$ receptor assay

Male SD rats were decapitated and their brains removed and placed on ice. The striatal tissue was dissected and homogenized with a glass homogenizer in 30 vol ice-cold TED buffer (50 mM Tris-HCl, 1 mM EDTA, 1 mM dithiothreitol, pH 7.4). Next, the homogenate was centrifuged at 21,000*g* for 30 min at 4°C. The pellet was suspended in 30 vol TED buffer (pH 7.4) and incubated in a water bath for 10 min at 37°C to remove endogenous ligands. The suspension was centrifuged again at 21,000*g* for 30 min at 4°C. The pellet was resuspended in 30 vol TED buffer (pH 7.4) and the centrifugation step was repeated. The final pellet was suspended in 10 vol 50 mM Tris-HCl (pH 7.4) and stored at −80°C until use. For the D$_2$ receptor antagonist [^{35}S]GTPγS assay, 15 μg/ml of striatal homogenate was incubated in triplicate with 0.8 nM [^{35}S]GTPγS in an assay buffer (50 mM Tris-HCl, pH 7.4, 1 mM EGTA, 3 mM $MgCl_2$, 100 mM NaCl, 0.1 mM dithiothreitol, 500 μM ascorbic acid, 20 μM GDP, and 100 μM dopamine) in the presence of increasing concentrations of the tested compounds (10^{-9} to 10^{-5} M). The effect on the basal G-protein activation threshold was determined in assay buffer deprived of dopamine. The final dimethyl sulfoxide (DMSO) concentration in the assay was 5%. Dopamine was dissolved in 50 mM Tris buffer (pH 7.4) supplemented with 500 μM ascorbic acid to prevent oxidation. Nonspecific binding was determined with 100 μM of unlabeled GTPγS. The reaction mixture was incubated for 60 min at 30°C at a volume of 250 μl. Next, 96-well Unifilter Plates were presoaked for 1 h with 50 mM Tris-HCl (pH 7.4) before harvesting. The reaction was terminated by vacuum filtration on filter plates with the FilterMate Harvester. The samples were then rapidly washed with 2 ml of 50 mM Tris-HCl (pH 7.4) buffer. Filter plates were dried for 2 h at 50°C. After drying, 45 μl of EcoScint-20 scintillant was added to the wells. Radioactivity was counted in a Trilux MicroBeta^2 counter. Data were analyzed with GraphPad Prism 5.0 software. Curves were fitted with a one-site nonlinear regression model. Potency (pIC_{50} and pK_B) and efficacy (E_{max}) were calculated from the Cheng–Prusoff and Gaddum/Schild models and expressed as mean ± *SEM*.

4.3 | Computational methods

4.3.1 | Compound preparation

The studied compounds **3a**–**n** and **4a**–**n** were modeled using the LigPrep module[52] of Schrödinger suite of software, v. 2019-4 as previously reported.[22–26] Both enantiomers regarding the configuration of the hydroxyl group were modeled, if applicable. To identify the protonation state, the Epik module[53] of Schrödinger suite of software, v. 2019-4 was applied.

4.3.2 | Receptor structures

In the cases when receptor X-ray structures were available, they were taken for molecular docking after necessary mutations: serotonin 5-HT$_{2A}$ receptor in complex with the antagonist risperidone (PDB ID: 6A93[54]) and serotonin 5-HT$_{2C}$ receptor in complex with the inverse agonist ritanserin (PDB ID: 6BQH[27]). In the case of

serotonin 5-HT_{1A} receptor, the previously published homology model was used.[23] All receptor models were in an inactive conformation. The structures of the biomolecules were preprocessed using the Protein Preparation Wizard of Maestro Release 2019.4[55] to optimize the hydrogen bonding network and to remove any possible artifacts as reported previously.[56]

4.3.3 | Molecular docking

Standard Precision (SP) approach of Glide[57] from Schrödinger release 2019-4 was used for molecular docking of the studied compounds to receptor models, as reported previously.[22–26] The grid files were generated on the basis of co-crystallized or co-modeled ligand. The hydroxyl groups of the following residues of the active sites were made flexible: Tyr96 (2.63), Thr121 (3.37), Ser168 (4.57), Thr188 (extracellular loop 2, ecl2), Ser190 (ecl2), Tyr195 (5.39), Thr196 (5.40), Ser199 (5.43), Thr200 (5.44), Tyr390 (7.42) for serotonin 5-HT_{1A} receptor; Ser131 (2.60), Thr134 (2.63), Ser159 (3.36), Ser207 (4.57), Ser226 (ecl2), Tyr370 (7.42) for serotonin 5-HT_{2A} receptor; and Ser 110 (2.60), Tyr118 (ecl1), Thr 206 (ecl2), Tyr358 (7.42) for serotonin 5-HT_{2C} receptor (numbers in parenthesis indicate GPCRdb generic numbers[58]). Twenty poses were generated for each receptor and each compound. The final poses were selected based on Glide docking scores and visual inspection among the poses where the protonatable nitrogen atom of the ligand interacted with conserved Asp 3.32. Visualization of molecular modeling results was achieved with Maestro Release 2019.4[55] and PyMol 2.0.4[59] software. NCI maps of ligand–receptor interactions were computed with NCIPlot v. 3.0[60] at the distance below 4 Å from the ligand and visualized with VMD v. 1.9.1,[61] as reported earlier.[62]

4.4 | In vivo behavioral tests

4.4.1 | General procedures

The studies were conducted on male Albino Swiss mice (18–23 g). The mice were housed in cages, five individuals per cage in environmentally controlled rooms (ambient temperature 22 ± 1°C; relative humidity 50–60%; 12-h light/dark cycle, lights on at 8:00). Standard laboratory food (LSM; Agropol-Motycz) and filtered water were available ad libitum. All the experimental procedures were carried out according to the National Institute of Health Guidelines for the Care and Use of Laboratory Animals and the European Community Directive for the Care and Use of Laboratory Animals of November 24, 1986 (86/609/EEC), and approved by the Local Ethics Committee for Animal Experimentation.

The investigated compounds (**3b**, **3e**, **4a**, **4j**, **4n**) in all tests were administered intraperitoneally, dissolved in DMSO (final concentration of 0.1%), and then diluted by aqueous solution of 0.5% methylcellulose (tylose) and injected 60 min before the tests. Other drugs (amphetamine [amph], MK-801, buspirone, fluoxetine) were administered intraperitoneally diluted in saline and injected 30 min (amph), 60 min (buspirone, fluoxetine), or immediately (MK-801 for hyperactivity test) before the tests. All compounds were given in a volume of 10 ml/kg to mice. The control animals received an equivalent volume of the solvent at the respective time before the tests. In the PA test, MK-801 was administered 15 min after administration of the compounds.

All the experiments were conducted in the light phase between 09.00 a.m. and 14.00 p.m. The experiments were performed by an observer unaware of the treatment administered.

4.4.2 | Spontaneous locomotor activity, amphetamine- and MK-801-induced hyperactivity

The locomotor activity of mice was measured using an animal activity meter Opto-Varimex-4 Auto-Track (Columbus Instruments). This automatic device consists of eight transparent cages with a lid, set of four infrared emitters (each emitter has 16 laser beams), and eight detectors monitoring animal movements. To assess the spontaneous activity of mice, the compounds or vehicles (as a control) were administered 60 min before the test. In another set of experiments, the influence of tested compounds on amph- and MK-801-induced hyperactivity in mice was evaluated. The study was conducted in the same apparatus, but each mouse received amph (5 mg/kg, sc) 30 min after injection of vehicle or tested compounds, or MK-801 (0.3 mg/kg, ip) 60 min after or immediately before the test. The animals were placed in the cage individually, 50 min after the administration of the tested compounds, for a period of 10 min for acclimatization. After this time, their activity was noted after 6 min (corresponded with the time duration of the FST and close [5 min] to the EPM test, respectively) and after 20 min, to observe the dynamics of changes. The distance traveled in centimeters was measured. The cages were cleaned up with 10% ethanol after each mouse trial.

4.4.3 | Motor coordination

The effects of investigated compounds on motor coordination were evaluated in the rotarod[63] and chimney[64] tests. In the first test, motor impairments were measured, defined as the inability to maintain balance on a rotating rod (at a constant speed of 18 rpm) for 1 min. In the second test, motor impairments were assessed by the inability of the mouse to climb up the tube backward (3 cm in inner diameter, 25 cm long) within 60 s. Before the tests, the animals were trained once a day for 3 days. The animals that were able to stay on the rotating rod or to leave the chimney for 60 s were approved for experiments.

4.4.4 | FST (Porsolt's test) in mice

The experiment was carried out according to the method of Porsolt et al.[65] Mice were individually placed in a glass cylinder (25 cm high;

10 cm in diameter) containing water maintained at 23–25°C, and they were left there for 6 min. The total duration of immobility was recorded during the last 4 min of a 6-min test session. A mouse was regarded as immobile when it remained floating on the water, making only small movements to keep its head above the water.

4.4.5 | EPM test

The EPM studies were carried out on mice according to the method of Lister.[66] The EPM apparatus was made of plexiglass and consisted of two open (30 × 5 cm) and two enclosed (30 × 5 × 15 cm) arms. The arms extended from a central platform of 5 × 5 cm. The apparatus was mounted on a plexiglass base, raising it 38.5 cm above the floor, and illuminated by a red light. The test consisted of placing a mouse at the center of the apparatus (facing an open arm) and allowing it to freely explore. The number of entries into the open arms and the time spent in these arms were scored for a 5-min test period. An entry was defined as placing all four paws within the boundaries of the arm. The following measures were obtained from the test: the total number of arm entries; the percentage of arm entries into the open arms; and the time spent in the open arms expressed as a percentage of the time spent in both the open and closed arms. Anxiolytic activity was indicated by increases in the time spent in open arms and in the number of open arm entries. The total number of entries into either type of arm was used additionally as a measure of the overall motor activity.

4.4.6 | Bar test

Catalepsy was measured using the bar test 60 min after drug administration: the front paws of each subject were placed on a cylindrical metal bar (0.75 cm diameter) that was elevated 4.5 cm above the table. The time during which both forelimbs remained on the bar was recorded up to a maximum of 30 s. The test was repeated three times (intertrial interval: 1 min). Animals were put back in their home cage after each measurement of catalepsy. Mice that remained motionless with their paws on the bar for 10 s (with the exception of respiratory movements) were scored as cataleptic.[67]

4.4.7 | PA test

The PA apparatus consists of a two-compartment acrylic box with a lighted compartment (10 × 13 × 15 cm) and a darkened compartment (25 × 20 × 15 cm). The light chamber was illuminated by a fluorescent light (8 W) and was connected to the dark chamber that was equipped with an electric grid floor. Entry of animals to the dark box was punished by an electric foot shock (0.2 mA for 2s).

On the first day of training (pre-test), all mice were allowed to habituate in the experimental room for at least 30 min before the experiments. Each animal was then gently placed in the light compartment of the apparatus and allowed to explore the light box. After 30 s, the guillotine door was opened, and the mouse was allowed to enter the dark compartment. When the mice entered the dark compartment, the guillotine door was closed and an electric foot shock (0.2 mA) of 2 s duration was delivered immediately to the animal via the grid floor of the dark room by an insulated stimulator. The latency with which the animal crossed into the dark compartment was recorded (TL1). After 20 s, the animal was removed from the apparatus and placed temporarily in its home cage. If the mouse failed to enter the dark box within 300 s, it was placed into this dark box, the door was closed, and electric foot shock was delivered to the animal. In this case, TL1 value was recorded as 300 s. After 24 hours, in the subsequent trial (retention), the same mice were again placed individually in the light compartment of the PA apparatus. After a 30 s adaptation period in the light (safe) chamber, the guillotine door was opened and the time taken to re-enter the dark compartment was recorded (TL2). No foot shock was applied in this trial. If the animal did not enter the dark chamber within 300 s, the retention test was terminated and TL2 was recorded as 300 s. No foot shock was applied in this trial.

In this experiment, the effect of **3b**, **3e**, **4a**, **4j**, and **4n** on the consolidation of the passive avoidance response in mice was examined. All compounds were given immediately after the first trial, and 15 min later, MK-801 (0.3 mg/kg, ip) was administered.

For the memory-related behaviors, the changes in PA performance were expressed as the difference between retention and training latencies, which was taken as LI. LI was calculated for each animal as the ratio: LI = (TL2 − TL1)/TL1. TL1 is the time taken to enter the dark compartment during the training and TL2 is the time taken to re-enter the dark compartment during the retention.[51]

4.4.8 | Statistical analysis

The results were calculated by the one-way analysis of variance, followed by Dunnett's post hoc test. The results are presented as mean ± *SEM*. The level of $p < .05$ was considered as statistically significant. All the figures were prepared by the GraphPad Prism version 5.00 for Windows.

4.5 | Ex vivo assays

4.5.1 | General procedures

Male rats (SD, 160–200 g; Harlan Laboratories) were manipulated and cared for in strict compliance with the *Principles of Laboratory Animal Care* (NIH publication no. 86–23, revised 1985) and the Italian D.L. no. 116 of January 27, 1992, and associated guidelines in the European Communities Council Directive of November 24, 1986 (86/609/ECC). Animal housing complied with recent pharmacological guidance.[68] All animals weighing 160–200 g were used after a 1-week acclimation period (temperature 23 ± 2°C; humidity 60%, free access to water, and standard food).

4.5.2 | Ileum preparation and evaluation of 5-HT-evoked contractions

Rats were asphyxiated using CO_2, and segments (1–1.5 cm) of ileum were removed, flushed of luminal contents, and placed in Krebs solution (119 mM NaCl, 4.75 mM KCl, 1.2 mM KH_2PO_4, 25 mM $NaHCO_3$, 2.5 mM $CaCl_2$, 1.5 mM $MgSO_4$, and 11 mM glucose). The segments were prepared as previously described[51]: the segments were set up in such a way as to record contractions mainly from the longitudinal axis, in an organ bath containing 20 ml of Krebs solution, bubbled with 95% O_2 and 5% CO_2, and maintained at 37°C. The tissues were connected to an isotonic transducer (load: 0.5 g), connected to a PowerLab system (Ugo Basile). Ileal segments were equilibrated for 60 min,[19] followed by three repeated additions of submaximal concentration of 5-HT (10^{-5} M) to record stable control contractions. To evaluate the inhibitory activity, the responses were observed in the presence of increasing concentrations (10^{-8} to 10^{-5} M). In preliminary experiments, the effect of 5-HT was observed in the presence of the neuronal blocker tetrodotoxin (0.3 μM), the muscarinic receptor antagonist atropine (1 μM), the adrenergic receptor antagonist phentolamine (10^{-6} M) plus propranolol (10^{-6} M), and the 5-HT_{2A} antagonist ketanserin (0.1 μM). The contact time for each concentration was 10 min. The compounds were dissolved in DMSO. DMSO (<0.01%) did not modify 5-HT-induced contractions. Results are expressed as mean (*SEM*). The concentration of the compounds that produced 50% inhibition of 5-HT-induced contractions (IC_{50}) or maximal inhibitory effect (E_{max}) was used to characterize compounds' potency and efficacy, respectively. The IC_{50} and E_{max} values were calculated with the aid of a computer program (GraphPad Prism 5).

ACKNOWLEDGMENTS

The NMR spectral data were provided by Centro di Ricerca Interdipartimentale di Analisi Strumentale, Università degli Studi di Napoli "Federico II." The assistance of the staff is gratefully appreciated. Calculations were partially performed under a computational grant by the Interdisciplinary Center for Mathematical and Computational Modeling (ICM), Warsaw, Poland (Grant Number G30-18), and under resources and licenses from CSC, Finland. The authors sincerely thank Agata Pawłowska for the technical performance of the radioligand binding assay. Radioligand binding studies were carried out with the use of the Center for Preclinical Research and Technology, Medical University of Warsaw infrastructure.

CONFLICTS OF INTERESTS

The authors declare that there are no conflicts of interests.

ORCID

Ferdinando Fiorino http://orcid.org/0000-0001-7357-5751

REFERENCES

[1] W. Quaglia, C. Cifani, F. Del Bello, M. Giannella, G. Giorgioni, M. V. Micioni Di Bonaventura, A. Piergentili, *Serotonin—A Chemical Messenger Between All Types of Living Cells*, InTechOpen, **2017**, p. 67, Ch. 4.

[2] A. Ju, B. Fernandez-Arroyo, Y Wu, D. Jacky, A. Beyeler, *Mol. Brain* **2020**, *13*, 99. https://doi.org/10.1186/s13041-020-00605-5

[3] A. Corvino, F. Fiorino, B. Severino, I. Saccone, F. Frecentese, E. Perissutti, P. Di Vaio, V. Santagada, G. Caliendo, E. Magli, *Curr. Med. Chem.* **2018**, *25*(*27*), 3214.

[4] D. E. Nichols, C. D. Nichols, *Chem. Rev.* **2008**, *108*, 1614.

[5] D. Hoyer, J. P. Hannon, G. R. Martin, *Pharmacol. Biochem. Behav.* **2002**, *71*, 533.

[6] M. Bancila, D. Verge, O. Rampin, J. R. Backstrom, E. Sanders-Bush, K. E. McKenna, L. Marson, A. Calas, F. Giuliano, *Neuroscience* **1999**, *92*(*4*), 1523.

[7] Y. Kimura, K. Hatanaka, Y. Naitou, K. Maeno, I. Shimada, A. Koakutsu, F. Wanibuchi, T. Yamaguchi, *Eur. J. Pharmacol.* **2004**, *483*(*1*), 37.

[8] K. Kucwaj-Brysz, R. Kurczab, E. Zeslawska, A. Lubelska, M. A. Marc, G. Latacz, G. Satala, W. Nitek, K. Kiec-Kononowicz, J. Handzlik, *MedChemComm* **2018**, *9*,1033.

[9] G. Caliendo, F. Fiorino, P. Grieco, E. Perissutti, V. Santagada, B. Severino, G. Bruni, M. R. Romeo, *Bioorg. Med. Chem.* **2000**, *8*, 533.

[10] (a) G. Caliendo, F. Fiorino, E. Perissutti, B. Severino, S. Gessi, E. Cattabriga, P. A. Borea, V. Santagada, *Eur. J. Med. Chem.* **2001**, *36*(*11–12*), 873.; (b) G. Caliendo, F. Fiorino, E. Perissutti, B. Severino, D. Scolaro, S. Gessi, E. Cattabriga, P. A. Borea, V. Santagada, *Eur. J. Pharm. Sci.* **2002**, *16*, 15.

[11] F. Fiorino, E. Perissutti, B. Severino, V. Santagada, D. Cirillo, S. Terracciano, P. Massarelli, G. Bruni, E. Collavoli, C. Renner, G. Caliendo, *J. Med. Chem.* **2005**, *48*, 5495.

[12] F. Fiorino, B. Severino, F. De Angelis, E. Perissutti, F. Frecentese, P. Massarelli, G. Bruni, E. Collavoli, V. Santagada, G. Caliendo, *Arch. Pharm. (Weinheim)* **2008**, *341*, 20.

[13] F. Fiorino, B. Severino, F. De Angelis, E. Perissutti, E. Magli, F. Frecentese, A. Esposito, P. Massarelli, C. Nencini, B. Viti, V. Santagada, G. Caliendo, *Pharmazie* **2009**, *64*(*9*), 555.

[14] F. Fiorino, B. Severino, F. De Angelis, E. Perissutti, E. Magli, F. Frecentese, A. Esposito, P. Massarelli, C. Nencini, V. Santagada, G. Caliendo, *Bioorg. Med. Chem. Lett.* **2010**, *20*(*9*), 2978.

[15] F. Fiorino, B. Severino, E. Magli, E. Perissutti, F. Frecentese, A. Esposito, G. M. Incisivo, A. Ciano, P. Massarelli, C. Nencini, V. Santagada, G. Caliendo, *Eur. J. Med. Chem.* **2012**, *47*, 520.

[16] (a) F. Fiorino, A. Ciano, E. Magli, B. Severino, A. Corvino, E. Perissutti, F. Frecentese, P. Di Vaio, A. A. Izzo, R. Capasso, P. Massarelli, C. Nencini, I. Rossi, E. Kedzierska, J. Orzelska-Gòrka, A. Bielenica, V. Santagada, G. Caliendo, *Eur. J. Med. Chem.* **2016**, *110*, 133.; (b) Bielenica, A., E. Kedzierska, M. Kolinski, S. Kmiecik, A. Kolinski, F. Fiorino, B. Severino, E. Magli, A. Corvino, I. Rossi, P. Massarelli, A. E. Koziol, A. Sawczenko, M. Struga, *Eur. J. Med. Chem.* **2016**, *116*, 173.

[17] F. Fiorino, E. Magli, E. Kedzierska, A. Ciano, A. Corvino, B. Severino, E. Perissutti, F. Frecentese, P. Di Vaio, I. Saccone, A. A. Izzo, R. Capasso, P. Massarelli, I. Rossi, J. Orzelska-Gòrka, J. H. Kotlinska, V. Santagada, G. Caliendo, *Bioorg. Med. Chem.* **2017**, *25*(*20*), 5820.

[18] F. Fiorino, E. Magli, B. Severino, A. Corvino, A. Ciano, E. Perissutti, F. Frecentese, P. Massarelli, C. Nencini, V. Santagada, G. Caliendo, *Arch. Pharm. (Weinheim)* **2014**, *347*(*10*), 698.

[19] M. R. Briejer, C. Mathis, J. A. Schuurkes, *Neurogastroenterol. Motil.* **1997**, *9*(*4*), 231.

[20] A. A. Kaczor, E. Rutkowska, D. Bartuzi, K. M. Targowska-Duda, D. Matosiuk, J. Selent, *Methods Cell Biol.* **2016**, *132*, 359.

[21] D. Bartuzi, A. A. Kaczor, K. M. Targowska-Duda, D. Matosiuk, *Molecules* **2017**, *22*, 340.

[22] A. A. Kaczor, A. G. Silva, M. I. Loza, P. Kolb, M. Castro, A. Poso, *ChemMedChem* **2016**, *11*, 718.

[23] A. A. Kaczor, K. M. Targowska-Duda, B. Budzyńska, G. Biała, A. G. Silva, M. Castro, *Neurochem. Int.* **2016**, *96*, 84.

[24] A. A. Kaczor, M. Jörg, B. Capuano, *J. Mol. Model.* **2016**, *22*(*203*), 1.

[25] M. Kondej, T. M. Wróbel, A. G. Silva, P. Stępnicki, O. Koszła, E. Kędzierska, A. Bartyzel, G. Biała, D. Matosiuk, M. I. Loza, M. Castro, A. A. Kaczor *Eur. J. Med. Chem.* **2019**, *180*, 673.
[26] M. Kondej, A. Bartyzel, M. Pitucha, T. M. Wróbel, A. G. Silva, D. Matosiuk, M. Castro, A. A. Kaczor, *Molecules* **2018**, *23*, 2249.
[27] Y. Peng, J. D. McCorvy, K. Harpsøe, K. Lansu, S. Yuan, P. Popov, L. Qu, M. Pu, T. Che, L. F. Nikolajsen, X. P. Huang, Y. Wu, L. Shen, W. E. Bjørn-Yoshimoto, K. Ding, D. Wacker, G. H. Han, J. Cheng, V. Katritch, A. A. Jensen, M. A. Hanson, S. Zhao, D. E. Gloriam, B. L. Roth, R. C. Stevens, Z.-J. Liu, *Cell* **2018**, *172*, 719.
[28] B. F. Seibet, A. C. Schiedel, D. Thimm, S. Hinz, F. F. Sherbiny, C. E. Muller. *Biochem. Pharmacol.* **2013**, *85*, 1317.
[29] M. Wheatley, D. Wootten, M. Conner, J. Simms, R. Kendrick, R. Logan, D. Poyner, J. Barwell, *Br. J. Pharmacol.* **2012**, *165*, 1688.
[30] S.-M. Lee, J. M. Booe, A. A. Pioszak, *Eur. J. Pharmacol.* **2015**, *763*, 196.
[31] A. Zagórska, M. Kołaczkowski, A. Bucki, A. Siwek, G. Kazek, G. Satała, A. J. Bojarski, A. Partyka, A. Wesołowska, M. Pawłowski, *Eur. J. Med. Chem.* **2015**, *97*, 142.
[32] A. Partyka, R. Kurczab, V. Canale, G. Satała, K. Marciniec, A. Pasierb, M. Jastrzębska-Więsek, M. Pawłowski, A. Wesołowska, A. J. Bojarski, P. Zajdel, *Bioorg. Med. Chem.* **2017**, *25*, 3638.
[33] S. Podlewska, R. Kafel, E. Lacivita, G. Satała, A. J. Kooistra, M. Vass, C. de Graaf, M. Leopoldo, A. J. Bojarski, S. Mordalski, *Eur. J. Med. Chem.* **2018**, *151*, 797.
[34] E. Magli, E. Kędzierska, A. A. Kaczor, B. Severino, A. Corvino, E. Perissutti, F. Frecentese, I. Saccone, P. Massarelli, E. Gibuła-Tarłowska, J. H. Kotlinska, V. Santagada, G. Caliendo, F. Fiorino, *Arch. Pharm. (Weinheim)* **2019**, *352*, 1.
[35] (a) E. R. Johnson, S. Keinan, P. Mori-Sánchez, J. Contreras-García, A. J. Cohen, W. Yang, *J. Am. Chem. Soc.* **2010**, *132*, 6498.; (b) A. N. Bootsma, A. C. Doney, S. Wheeler, *J. Am. Chem. Soc.* **2019**, *141*(*28*), 11027.; (c) S. E. Wheeler, *Acc. Chem. Res.* **2013**, *46*(*4*), 1029.
[36] H. G. Vogel, *Drug Discovery and Evaluation: Pharmacological Assays* (Ed: H. Vogel), Springer-Verlag, Berlin Heidelberg **2008**, p. 565.
[37] P. H. Gobira, J. Ropke, D. C. Aguiar, J. A. Crippa, F. A. Moreira, *Rev. Bras. Psiquiatr.* **2013**, *35*(*2*), 132.
[38] C. A. Jones, D. J. G. Watson, K. C. F. Fone, *Br. J. Pharmacol.* **2011**, *164*, 1162.
[39] J. H. Kim, P. Vezina, *Pharmacol. Biochem. Behav.* **2002**, *73*(*2*), 333.
[40] H. Y. Meltzer, *Neuropsychopharmacology* **1999**, *21*, 106S.
[41] X. López Hill, A. Richeri, M. C. Scorza, *Physiol. Behav.* **2017**, *17*, 346.
[42] M. Tomić, D. Ignjatović, G. Tovilović, D. Andrić, G. Roglić, S. Kostić-Rajacić, *Bioorg. Med. Chem. Lett.* **2007**, *17*, 5749.
[43] S. Leucht, C. Corves, D. Arbter, R. R. Engel, C. Li, J. M. Davis, *Lancet* **2009**, *373*, 31.
[44] P. Chopin, M. Briley, *Psychopharmacology (Berl.)* **1993**, *110*(*4*), 409.
[45] S. Pellow, P. Chopin, S. E. File, M. Briley, *J. Neurosci. Methods* **1985**, *14*(*3*), 149.
[46] K. Harada, M. Aota, T. Inoue, R. Matsuda, T. Mihara, T. Yamaji, K. Ishibashi, N. Matsuoka, *Eur. J. Pharmacol.* **2006**, *553*(*1–3*), 171.
[47] D. C. Hoffman, H. Donovan, *Psychopharmacology* **1995**, *120*, 128.
[48] G. Di Giovanni, P. De Deurwaerdère, *Pharmacol. Ther.* **2016**, *157*, 125.
[49] R. S. Kahn, *Neuropsychiatria i Neuropsychologia* **2014**, *9*(*2*), 41.
[50] A. Bucki, M. Marcinkowska, J. Śniecikowska, K. Więckowski, M. Pawłowski, M. Głuch-Lutwin, A. Gryboś, A. Siwek, K. Pytka, M. Jastrzębska-Więsek, A. Partyka, A. Wesołowska, P. Mierzejewski, M. Kołaczkowski, *J. Med. Chem.* **2017**, *60*(*17*), 7483.
[51] M. Javadi-Paydar, M. Zakeri, A. Norouzi, H. Rastegar, N. Mirazi, A. R. Dehpour, *Brain Res.* **2012**, *1429*, 61.
[52] Schrödinger Release 2019-4: LigPrep, Schrödinger, LLC, New York, NY **2019**.
[53] Schrödinger Release 2019-4: Epik, Schrödinger, LLC, New York, NY **2019**.
[54] K. T. Kimura, H. Asada, A. Inoue, F. M. N. Kadji, D. Im, C. Mori, T. Arakawa, K. Hirata, Y. Nomura, N. Nomura, J. Aoki, S. Iwata, T. Shimamura, *Nat. Struct. Mol. Biol.* **2019**, *26*, 121.
[55] Schrödinger Release 2019-4: BioLuminate, Schrödinger, LLC, New York, NY **2019**.
[56] J. Z. Patel, T. Parkkari, T. Laitinen, A. A. Kaczor, S. M. Saario, J. R. Savinainen, D. Navia-Paldanius, M. Cipriano, J. Leppänen, I. O. Koshevoy, A. Poso, C. J. Fowler, J. T. Laitinen, T. Nevalainen, *J. Med. Chem.* **2013**, *56*, 8484.
[57] R. A. Friesner, R. B. Murphy, M. P. Repasky, L. L. Frye, J. R. Greenwood, T. A. Halgren, P. C. Sanschagrin, D. T. Mainz, *J. Med. Chem.* **2006**, *49*, 6177.
[58] G. Pándy-Szekeres, C. Munk, T. M. Tsonkov, S. Mordalski, K. Harpsøe, A. S. Hauser, A. J. Bojarski, D. E. Gloriam, *Nucleic Acids Res.* **2018**, *46*, D440.
[59] The PyMOL Molecular Graphics System, Version 2.0 Schrödinger, LLC.
[60] J. Contreras-García, E. R. Johnson, S. Keinan, R. Chaudret, J. P. Piquemal, D. N. Beratan, W. Yang, *J. Chem. Theory Comput.* **2011**, *7*, 625.
[61] W. Humphrey, A. Dalke, K. Schulten, *J. Mol. Graphics* **1996**, *14*, 33.
[62] M. Pitucha, K. Sobotka-Polska, R. Keller, A. Pachuta-Stec, E. Mendyk, A. A. Kaczor, *J. Mol. Struct.* **2016**, *1104*, 24.
[63] F. Gross, J. Tripod, R. Meir, *Schweiz. Med. Wochschr.* **1955**, *85*, 305.
[64] J. R. Boissier, J. Tardy, J. C. Diverres, Med. *Exp. (Basel)*, **1960**, 3, 81.
[65] R. D. Porsolt, A. G. Blavet, M. Jalfre, *Eur. J. Pharmacol.* **1978**, *47*, 379.
[66] R. G. Lister, *Psychopharmacology* **1987**, *92*, 180.
[67] P. J. Little, D. R. Compton, M. R. Johnson, L. S. Melvin, B. R. Martin, *J. Pharmacol. Exp. Ther.* **1988**, *247*(*3*), 1046.
[68] M. J. Curtis, R. A. Bond, D. Spina, A. Ahluwalia, S. P. A. Alexander, M. A. Giembycz, A. Gilchrist, D. Hoyer, P. A. Insel, A. A. Izzo, A. J. Lawrence, D. J. MacEwan, L. Moon, S. Wonnacott, A. H. Weston, J. C. McGrath, *Br. J. Pharmacol.* **2015**, *172*(*14*), 3461.

SUPPORTING INFORMATION

Additional Supporting Information may be found online in the supporting information tab for this article.

How to cite this article: Magli E, Kędzierska E, Kaczor AA, et al. Synthesis, docking studies, and pharmacological evaluation of 2-hydroxypropyl-4-arylpiperazine derivatives as serotoninergic ligands. *Arch Pharm*. 2021;354:e2000414. https://doi.org/10.1002/ardp.202000414